Anharmonicity and mode-mode coupling effects analyzed by four-wave-mixing photon-echo spectroscopy

K. K. Liang[1,*] and A. A. Villaeys[1,2]

[1]*Research Center for Applied Sciences, Academia Sinica, Taipei 115, Taiwan, and Department of Biochemical Science and Technology, National Taiwan University, Taipei 106, Taiwan*

[2]*Université de Strasbourg and Institut de Physique et Chimie des Matériaux de Strasbourg, Strasbourg, France*

(Received 6 May 2010; published 30 July 2010)

The present work is devoted to the description of a nonperturbative treatment of anharmonic effect and mode-mode coupling taking place in molecular vibrational systems. The information is obtained from the four-wave-mixing signal detected in the usual photon-echo phase-matched direction, termed 4WM photon-echo, using heterodyne detection to test separately the real and the imaginary parts of the third-order polarization. This approach allows a complete redistribution of the relaxation, dephasing, and transition constants on account of the magnitude of the coupling strength. In addition, our analytical approach accounts for the contributions provided by the various possible chronological orderings of the field interactions. The high sensitivity of the signal with both the energy shifts induced by the internal couplings and off-resonant energy parameter of the laser excitation is properly analyzed in the framework of our analytical description.

DOI: 10.1103/PhysRevA.82.013423 PACS number(s): 42.50.Md, 82.53.Kp

I. INTRODUCTION

The traditional view of two- and three-pulse photon echo is based historically on two-level models undergoing slow and fast fluctuations, whose contributions to the linewidth have been analyzed in great detail. This picture allows well-defined roles to be assigned to the different contributions, which are classified as rephasing and non-rephasing terms and contribute to the third-order polarization created in the system by the three exciting laser beams [1,2]. Also, it has the advantage of giving a simple physical picture which retains the main processes occurring during the course of a photon-echo experiment. Today, photon-echo spectroscopy has a broader range of applications. To avoid unnecessary semantic discussions, we just mention that this terminology is used to describe either a signal consecutive to a rephasing process which can be solely obtained from systems undergoing large inhomogeneous broadening or, broadly speaking, as is the case in the present work, a coherent four-wave-mixing signal observed in the usual photon-echo phase-matched direction that is termed, throughout, the four-wave-mixing photon-echo signal. It is just this last signal which constitutes the starting point of the newly developed 2D spectroscopy obtained by a convenient double Fourier analysis of the time and delay time dependences of the signal [2–6].

Among the large variety of spectroscopic techniques, three-pulse photon echo has been extensively applied to study internal dynamical processes as diverse as energy transfer in photosynthetic complexes [7–10], solvation dynamics [11–13], and many others. More recently, a new variant of this technique sensitive to the correlated motion between different spectral excitation windows, termed two-color three-pulse photon-echo peak shift, has proven to be quite efficient to obtain information on the dynamics of strongly coupled multichromophoric systems and more specifically on their energy transfer [10–16]. An interesting aspect of this technique lies in the ability to directly probe the electronic coupling between the chromophores [17,18]. It is noteworthy to mention that when the time scale of energy transfer is comparable to the coherence time of the bath, non-Markovian effects enter into the dynamics and the description of the whole system has to be included properly into the description [16,19–23]. Besides, when the pulse durations become comparable either to the characteristic times driving the dynamical evolution or to the pulse delay times, using the impulse approximation method is not appropriate since various field orderings contribute significantly to the signal and they cannot be properly weighted by the overlaps of the laser pulses in the framework of this approximation.

In most of the ultrafast nonlinear spectroscopy experiments we are dealing with, the spectral broadening of the laser pulses is always quite large so that many levels of the molecular systems are involved because their energies fit within the spectral range. In our description, because the pulses are described analytically, all the contributions generated by the successive transitions leading to the third-order polarization are treated on the same footing and are properly weighted by the spectral overlaps between the pulses and the vibrational molecular resonances. In addition, all the various possible chronological orderings of the field interactions are accounted for.

Many experiments have suggested the peculiar role of the anharmonicity in the ground state, the nonlinear dependence of the transition dipole moment on the normal coordinates, or likewise the level-dependent dephasing dynamics. It has been shown that at least one of these processes is required to observe infrared optical nonlinearities [24–28]. In the present article, to study the peculiar roles played by anharmonicity and mode-mode coupling in the vibrational dynamics underlying a 4WM photon-echo (4WM PE) signal, we describe a three-pulse photon-echo experiment performed on a molecular

*Corresponding author: Research Center for Applied Sciences, Academia Sinica, 128, Section 2, Academia Road, Nankang, Taipei 115, Taiwan. E-mail address: kkliang@sinica.edu.tw.

system made of two oscillators undergoing anharmonity and mode-mode coupling. This type of vibrational model has been largely discussed in the literature where anharmonicity and mode-mode coupling have been handled perturbatively assuming that the main physical constants, say relaxation and dephasing constants as well as dipole moments, are not redistributed by the internal perturbations [5]. Here, because of the strong anharmonic coupling, a complete diagonalization is required. It implies not only a complete mixing of the energy levels but also a complete redistribution of the dipole moments as well as of the relaxation, transition, and dephasing constants among the eigenvibrational states. However, orientational effects are not considered here. Since orientational motions of the molecule in condensed phase are usually slower than vibrational motions, the orientational dynamics can be factorized and described independent of the internal dynamics. Notice that an extensive study of the role played by the orientational motion in third-order optical responses has been considered by Golonzka and Tokmakoff [29].

In Sec. II, we introduce the description of the vibrational system model made of two harmonic oscillators in the presence of a perturbation responsible for mode-mode coupling and anharmonicity. For strongly coupled systems, a perturbative approach is not appropriate because, first, higher order perturbation terms necessarily involve a large number of pathways and, second, if the perturbation is large, we must have a redistribution of all the dynamical constants participating in the evolution. Therefore, we introduce a global diagonalization of the levels, dipole moments, and dephasing and relaxation constants. Also, the evolution Liouvillians of the populations are evaluated, because the dynamics underlying the 4WM PE process populates some of the excited states. Next, in Sec. III, the third-order polarization is explicitly obtained in the photon-echo phase-matched direction and the signal is evaluated using heterodyne detection. The analytical description accounts for the laser pulse overlaps and the different chronological ordering of the laser excitations. Finally, in Sec. IV, a number of simulations are performed to emphasize the influence of anharmonicity and mode-mode coupling on the time dependence of the 4WM PE signal.

II. VIBRATIONAL MOLECULAR MODEL

The vibrational molecular model that we are dealing with is made of two interacting harmonic oscillators undergoing anharmonicity and mode-mode coupling. Therefore, its Hamiltonian involves three terms, say

$$\boldsymbol{H} = \boldsymbol{H}_{\mathrm{v}_1} + \boldsymbol{H}_{\mathrm{v}_2} + \boldsymbol{U}(\boldsymbol{Q}_1, \boldsymbol{Q}_2), \tag{II.1}$$

corresponding to two independent harmonic oscillators with Hamiltonians $\boldsymbol{H}_{\mathrm{v}_1}$ and $\boldsymbol{H}_{\mathrm{v}_2}$ associated with the normal coordinates $\boldsymbol{Q}_1$ and $\boldsymbol{Q}_2$, respectively, and their corresponding interaction $\boldsymbol{U}(\boldsymbol{Q}_1, \boldsymbol{Q}_2)$. The interaction term involves two contributions. The first one, denoted $\boldsymbol{U}_{\mathrm{anh}}(\boldsymbol{Q}_1, \boldsymbol{Q}_2)$, is responsible for anharmonicity and the second accounts for mode-mode coupling and is termed $\boldsymbol{U}_{\mathrm{coupl}}(\boldsymbol{Q}_1, \boldsymbol{Q}_2)$. They are given by the expressions

$$\boldsymbol{U}(\boldsymbol{Q}_1, \boldsymbol{Q}_2) = \boldsymbol{U}_{\mathrm{anh}}(\boldsymbol{Q}_1, \boldsymbol{Q}_2) + \boldsymbol{U}_{\mathrm{coupl}}(\boldsymbol{Q}_1, \boldsymbol{Q}_2), \tag{II.2}$$

with

$$\begin{aligned} \boldsymbol{U}_{\mathrm{anh}}(\boldsymbol{Q}_1, \boldsymbol{Q}_2) &= \frac{u_{111}}{6}\boldsymbol{Q}_1^3 + \frac{u_{222}}{6}\boldsymbol{Q}_2^3, \\ \boldsymbol{U}_{\mathrm{coupl}}(\boldsymbol{Q}_1, \boldsymbol{Q}_2) &= u_{12}\boldsymbol{Q}_1\boldsymbol{Q}_2 + \frac{u_{122}}{2}\boldsymbol{Q}_1\boldsymbol{Q}_2^2 + \frac{u_{112}}{2}\boldsymbol{Q}_1^2\boldsymbol{Q}_2. \end{aligned} \tag{II.3}$$

The matrix representation of the vibrational Hamiltonian in the basis of the individual harmonic modes involving ground state $|00\rangle$, singly excited states $|10\rangle$ and $|01\rangle$, overtones $|20\rangle$ and $|02\rangle$, and combination state $|11\rangle$ is deduced from the expression of the vibrational Hamiltonian including the anharmonic and mode-mode coupling terms $\boldsymbol{U}_{\mathrm{anh}}(\boldsymbol{Q}_1, \boldsymbol{Q}_2)$ and $\boldsymbol{U}_{\mathrm{coupl}}(\boldsymbol{Q}_1, \boldsymbol{Q}_2)$. Therefore, the vibrational Hamiltonian can be written as

$$\boldsymbol{H} = \begin{pmatrix} 0 & \frac{1}{2}(u_{122}+u_{111}) & \frac{1}{2}(u_{112}+u_{222}) & 0 & u_{12} & 0 \\ \frac{1}{2}(u_{122}+u_{111}) & \omega_1 & u_{12} & \frac{1}{\sqrt{2}}(u_{122}+2u_{111}) & \frac{1}{2}(3u_{112}+u_{222}) & \frac{1}{\sqrt{2}}u_{122} \\ \frac{1}{2}(u_{112}+u_{222}) & u_{12} & \omega_2 & \frac{1}{\sqrt{2}}u_{112} & \frac{1}{2}(3u_{122}+u_{111}) & \frac{1}{\sqrt{2}}(u_{112}+2u_{222}) \\ 0 & \frac{1}{\sqrt{2}}(u_{122}+2u_{111}) & \frac{1}{\sqrt{2}}u_{112} & 2\omega_1 & \sqrt{2}u_{12} & 0 \\ u_{12} & \frac{1}{2}(3u_{112}+u_{222}) & \frac{1}{2}(3u_{122}+u_{111}) & \sqrt{2}u_{12} & \omega_1+\omega_2 & \sqrt{2}u_{12} \\ 0 & \frac{1}{\sqrt{2}}u_{122} & \frac{1}{\sqrt{2}}(u_{112}+2u_{222}) & 0 & \sqrt{2}u_{12} & 2\omega_2 \end{pmatrix}, \tag{II.4}$$

where the state ordering $|00\rangle, |10\rangle, |01\rangle, |20\rangle, |11\rangle, |02\rangle$ is chosen in the order of their increasing energies for the sake of simplicity, by making the nonrestrictive assumption $\omega_1 < \omega_2$ for the numerical simulations. From the diagonalization of the vibrational Hamiltonian, we obtain a new representation denoted $\{|\epsilon_i\rangle\}$ with $i = 1$ to 6 based on the eigenstate problem $\boldsymbol{H}|\epsilon_i\rangle = \epsilon_i|\epsilon_i\rangle$ of the vibrational Hamiltonian. Both representations are illustrated in Fig. 1.

When the vibrational system of interest involves intermode couplings, as the one previously introduced in relations (II.2)

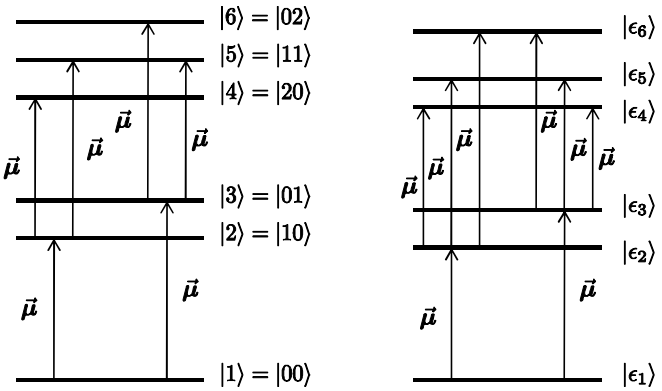

FIG. 1. Representation of the energy levels for the two vibrational modes with their corresponding dipole transition moments. On the left-hand side of the figure, the two harmonic modes are independent and the basis set $\{|ij\rangle\}$ is deduced from the zeroth-order harmonic oscillator states. On the right-hand side of the figure, due to anharmonic effect and mode-mode coupling, the eigenstate basis set $\{|\epsilon_j\rangle\}$ is used to describe the dynamics of the anharmonic and coupled oscillators. All the other allowed transitions have been neglected because of their negligible dipole moments.

and (II.3), the dynamics can be described in the local basis set and is then handled perturbatively. To account for the modifications of the relaxation, dephasing, and transition constants resulting from the anharmonic and mode-mode coupling terms, the diagonalization is required because, for increasing magnitudes of the perturbation terms, the first approach involves quite intricate combinations of pathways due to all possible orderings of the dipole and interaction terms. However, from the second approach based on diagonalization, the relaxation, dephasing, and transition constants need to be determined in the eigenstate basis set, and this is also true for the dipole moments. To this end, we start from the Liouvillian equation

$$\frac{\partial \boldsymbol{\rho}(t)}{\partial t} = -\frac{i}{\hbar}\boldsymbol{L}\boldsymbol{\rho}(t) - \boldsymbol{\Gamma}\boldsymbol{\rho}(t), \tag{II.5}$$

where $\boldsymbol{L}$ is the Liouvillian with respect to the vibrational Hamiltonian $\boldsymbol{H} = \boldsymbol{H}_{v_1} + \boldsymbol{H}_{v_2} + \boldsymbol{U}(\boldsymbol{Q}_1, \boldsymbol{Q}_2)$. As usual, $\boldsymbol{\Gamma}$ stands for the damping Liouvillian and $\boldsymbol{\rho}(t)$ for the density operator of the two anharmonic and coupled vibrational modes. In the local basis set, we have

$$\frac{\partial \boldsymbol{\rho}_{nm}(t)}{\partial t} = -\frac{i}{\hbar}\sum_{pq}\boldsymbol{L}_{nmpq}\boldsymbol{\rho}_{pq}(t) - \boldsymbol{\Gamma}_{mnpq}\boldsymbol{\rho}_{pq}(t), \tag{II.6}$$

and the same type of equation can be written in the eigenstate basis set:

$$\frac{\partial \boldsymbol{\rho}_{\alpha\beta}(t)}{\partial t} = -\frac{i}{\hbar}\sum_{\nu\lambda}\boldsymbol{L}_{\alpha\beta\nu\lambda}\boldsymbol{\rho}_{\nu\lambda}(t) - \boldsymbol{\Gamma}_{\alpha\beta\nu\lambda}\boldsymbol{\rho}_{\nu\lambda}(t). \tag{II.7}$$

Throughout, we use either Greek or Latin letters to refer to the zeroth-order basis set of the local harmonic modes or to the eigenstates of the anharmonic and coupled oscillators, respectively. From the transformation between the zeroth-order basis set and the eigenstate basis set, we get the following for the matrix representation of the Liouvillian:

$$\boldsymbol{\mathcal{L}}_{\alpha\beta\nu\lambda} = \sum_{tupq}\langle\alpha|t\rangle\langle u|\beta\rangle\langle p|\nu\rangle\langle\lambda|q\rangle\boldsymbol{\mathcal{L}}_{tupq}. \tag{II.8}$$

For the dipole moments, we have a similar relation given by

$$\langle\epsilon_i|\vec{\boldsymbol{\mu}}|\epsilon_j\rangle = \sum_{m,n}\langle\epsilon_i|m\rangle\langle n|\epsilon_j\rangle\vec{\boldsymbol{\mu}}_{mn}. \tag{II.9}$$

Once all these physical parameters driving the dynamics of the vibrational system are known, we can restate the dynamical evolution in the basis set $\{|\epsilon_j\rangle\}$ of the anharmonic and coupled vibrational modes. From Eq. (II.7), the time evolution of the coherences reduces to

$$\frac{\partial \boldsymbol{\rho}_{\alpha\beta}(t)}{\partial t} = -i\omega_{\alpha\beta}\boldsymbol{\rho}_{\alpha\beta}(t) - \boldsymbol{\Gamma}_{\alpha\beta\alpha\beta}\boldsymbol{\rho}_{\alpha\beta}(t), \tag{II.10}$$

while the corresponding equation for the population evolution is now expressed by

$$\frac{\partial \boldsymbol{\rho}_{\alpha\alpha}(t)}{\partial t} = -\sum_{\nu}\boldsymbol{\Gamma}_{\alpha\alpha\nu\nu}\boldsymbol{\rho}_{\nu\nu}(t). \tag{II.11}$$

Of course, because of the anharmonic and mode-mode coupling terms, most of the levels are coupled by transition constants and, in principle, all of them are allowed. Now, it is quite clear that for realistic values associated with these phenomena, as can be seen for instance from the spectra of coupled carbonyl stretches of $Rh(CO)_2(C_5H_7O_2)$ [30], some of these transition constants associated with the reverse transitions we evaluated are many orders of magnitude smaller than the other ones. Therefore, for the sake of simplicity, they are neglected from here on. Then, in the population Liouvillian subspace built from the eigenstate basis set, the damping Liouvillian can be expressed in the following form:

$$\boldsymbol{\Gamma} = \begin{pmatrix} 0 & \boldsymbol{\Gamma}_{\epsilon_1\epsilon_1\epsilon_2\epsilon_2} & \boldsymbol{\Gamma}_{\epsilon_1\epsilon_1\epsilon_3\epsilon_3} & \boldsymbol{\Gamma}_{\epsilon_1\epsilon_1\epsilon_4\epsilon_4} & \boldsymbol{\Gamma}_{\epsilon_1\epsilon_1\epsilon_5\epsilon_5} & \boldsymbol{\Gamma}_{\epsilon_1\epsilon_1\epsilon_6\epsilon_6} \\ 0 & \boldsymbol{\Gamma}_{\epsilon_2\epsilon_2\epsilon_2\epsilon_2} & \boldsymbol{\Gamma}_{\epsilon_2\epsilon_2\epsilon_3\epsilon_3} & \boldsymbol{\Gamma}_{\epsilon_2\epsilon_2\epsilon_4\epsilon_4} & \boldsymbol{\Gamma}_{\epsilon_2\epsilon_2\epsilon_5\epsilon_5} & \boldsymbol{\Gamma}_{\epsilon_2\epsilon_2\epsilon_6\epsilon_6} \\ 0 & \boldsymbol{\Gamma}_{\epsilon_3\epsilon_3\epsilon_2\epsilon_2} & \boldsymbol{\Gamma}_{\epsilon_3\epsilon_3\epsilon_3\epsilon_3} & \boldsymbol{\Gamma}_{\epsilon_3\epsilon_3\epsilon_4\epsilon_4} & \boldsymbol{\Gamma}_{\epsilon_3\epsilon_3\epsilon_5\epsilon_5} & \boldsymbol{\Gamma}_{\epsilon_3\epsilon_3\epsilon_6\epsilon_6} \\ 0 & 0 & 0 & \boldsymbol{\Gamma}_{\epsilon_4\epsilon_4\epsilon_4\epsilon_4} & \boldsymbol{\Gamma}_{\epsilon_4\epsilon_4\epsilon_5\epsilon_5} & \boldsymbol{\Gamma}_{\epsilon_4\epsilon_4\epsilon_6\epsilon_6} \\ 0 & 0 & 0 & \boldsymbol{\Gamma}_{\epsilon_5\epsilon_5\epsilon_4\epsilon_4} & \boldsymbol{\Gamma}_{\epsilon_5\epsilon_5\epsilon_5\epsilon_5} & \boldsymbol{\Gamma}_{\epsilon_5\epsilon_5\epsilon_6\epsilon_6} \\ 0 & 0 & 0 & 0 & \boldsymbol{\Gamma}_{\epsilon_6\epsilon_6\epsilon_5\epsilon_5} & \boldsymbol{\Gamma}_{\epsilon_6\epsilon_6\epsilon_6\epsilon_6} \end{pmatrix}_{\epsilon_1,\epsilon_2,\epsilon_3,\epsilon_4,\epsilon_5,\epsilon_6}, \tag{II.12}$$

where, to avoid any confusion, we have introduced the notation $\boldsymbol{\Gamma}_{\epsilon_i,\epsilon_j,\epsilon_k,\epsilon_l}$ for the eigenstate representation.

Identifying the integral representation of the density matrix with the definition of the population evolution Liouvillian we obtain

$$\begin{aligned}\boldsymbol{\rho}_{\alpha\alpha}(t) &= \frac{1}{2\pi i}\int_{-\infty+i\epsilon}^{\infty+i\epsilon} ds\, e^{st}[s\boldsymbol{I}+\boldsymbol{\Gamma}]^{-1}_{\alpha\alpha\nu\nu}\boldsymbol{\rho}_{\nu\nu}(t_0)\\ &= \sum_{\nu}\boldsymbol{G}_{\alpha\alpha\nu\nu}(t-t_0)\boldsymbol{\rho}_{\nu\nu}(t_0),\end{aligned} \tag{II.13}$$

and we require the evaluation of the inverse of $[s\boldsymbol{I}+\boldsymbol{\Gamma}]$. Once $\boldsymbol{\Gamma}$ is known, the Liouvillian $[s\boldsymbol{I}+\boldsymbol{\Gamma}]^{-1}$ can be calculated. Then, its inverse Laplace transform is obtained and according to Eq. (II.13) the evolution Liouvillians in the population subspace are deduced. They correspond to $\boldsymbol{G}_{\epsilon_1\epsilon_1\epsilon_1\epsilon_1}(t)=1$ for the ground state and

$$\begin{aligned}\boldsymbol{G}_{\epsilon_2\epsilon_2\epsilon_2\epsilon_2}(t) &= e^{-\frac{1}{2}(\boldsymbol{\Gamma}_{\epsilon_2\epsilon_2\epsilon_2\epsilon_2}+\boldsymbol{\Gamma}_{\epsilon_3\epsilon_3\epsilon_3\epsilon_3})t}\left[\cosh\left(\frac{t}{2}\left[\boldsymbol{\Gamma}^2_{\epsilon_2\epsilon_2\epsilon_2\epsilon_2}-2\boldsymbol{\Gamma}_{\epsilon_3\epsilon_3\epsilon_3\epsilon_3}\boldsymbol{\Gamma}_{\epsilon_2\epsilon_2\epsilon_2\epsilon_2}+\boldsymbol{\Gamma}^2_{\epsilon_3\epsilon_3\epsilon_3\epsilon_3}+4\boldsymbol{\Gamma}_{\epsilon_3\epsilon_3\epsilon_2\epsilon_2}\boldsymbol{\Gamma}_{\epsilon_2\epsilon_2\epsilon_3\epsilon_3}\right]^{\frac{1}{2}}\right)\right.\\ &\quad\left.+\frac{(-\boldsymbol{\Gamma}_{\epsilon_2\epsilon_2\epsilon_2\epsilon_2}+\boldsymbol{\Gamma}_{\epsilon_3\epsilon_3\epsilon_3\epsilon_3})\sinh\left(\frac{t}{2}\left[\boldsymbol{\Gamma}^2_{\epsilon_2\epsilon_2\epsilon_2\epsilon_2}-2\boldsymbol{\Gamma}_{\epsilon_3\epsilon_3\epsilon_3\epsilon_3}\boldsymbol{\Gamma}_{\epsilon_2\epsilon_2\epsilon_2\epsilon_2}+\boldsymbol{\Gamma}^2_{\epsilon_3\epsilon_3\epsilon_3\epsilon_3}+4\boldsymbol{\Gamma}_{\epsilon_3\epsilon_3\epsilon_2\epsilon_2}\boldsymbol{\Gamma}_{\epsilon_2\epsilon_2\epsilon_3\epsilon_3}\right]^{\frac{1}{2}}\right)}{\left[\boldsymbol{\Gamma}^2_{\epsilon_2\epsilon_2\epsilon_2\epsilon_2}-2\boldsymbol{\Gamma}_{\epsilon_3\epsilon_3\epsilon_3\epsilon_3}\boldsymbol{\Gamma}_{\epsilon_2\epsilon_2\epsilon_2\epsilon_2}+\boldsymbol{\Gamma}^2_{\epsilon_3\epsilon_3\epsilon_3\epsilon_3}+4\boldsymbol{\Gamma}_{\epsilon_3\epsilon_3\epsilon_2\epsilon_2}\boldsymbol{\Gamma}_{\epsilon_2\epsilon_2\epsilon_3\epsilon_3}\right]^{\frac{1}{2}}}\right],\\ \boldsymbol{G}_{\epsilon_3\epsilon_3\epsilon_3\epsilon_3}(t) &= e^{-\frac{1}{2}(\boldsymbol{\Gamma}_{\epsilon_2\epsilon_2\epsilon_2\epsilon_2}+\boldsymbol{\Gamma}_{\epsilon_3\epsilon_3\epsilon_3\epsilon_3})t}\left[\cosh\left(\frac{t}{2}\left[\boldsymbol{\Gamma}^2_{\epsilon_2\epsilon_2\epsilon_2\epsilon_2}-2\boldsymbol{\Gamma}_{\epsilon_3\epsilon_3\epsilon_3\epsilon_3}\boldsymbol{\Gamma}_{\epsilon_2\epsilon_2\epsilon_2\epsilon_2}+\boldsymbol{\Gamma}^2_{\epsilon_3\epsilon_3\epsilon_3\epsilon_3}+4\boldsymbol{\Gamma}_{\epsilon_3\epsilon_3\epsilon_2\epsilon_2}\boldsymbol{\Gamma}_{\epsilon_2\epsilon_2\epsilon_3\epsilon_3}\right]^{\frac{1}{2}}\right)\right.\\ &\quad\left.+\frac{(\boldsymbol{\Gamma}_{\epsilon_2\epsilon_2\epsilon_2\epsilon_2}-\boldsymbol{\Gamma}_{\epsilon_3\epsilon_3\epsilon_3\epsilon_3})\sinh\left(\frac{t}{2}\left[\boldsymbol{\Gamma}^2_{\epsilon_2\epsilon_2\epsilon_2\epsilon_2}-2\boldsymbol{\Gamma}_{\epsilon_3\epsilon_3\epsilon_3\epsilon_3}\boldsymbol{\Gamma}_{\epsilon_2\epsilon_2\epsilon_2\epsilon_2}+\boldsymbol{\Gamma}^2_{\epsilon_3\epsilon_3\epsilon_3\epsilon_3}+4\boldsymbol{\Gamma}_{\epsilon_3\epsilon_3\epsilon_2\epsilon_2}\boldsymbol{\Gamma}_{\epsilon_2\epsilon_2\epsilon_3\epsilon_3}\right]^{\frac{1}{2}}\right)}{\left[\boldsymbol{\Gamma}^2_{\epsilon_2\epsilon_2\epsilon_2\epsilon_2}-2\boldsymbol{\Gamma}_{\epsilon_3\epsilon_3\epsilon_3\epsilon_3}\boldsymbol{\Gamma}_{\epsilon_2\epsilon_2\epsilon_2\epsilon_2}+\boldsymbol{\Gamma}^2_{\epsilon_3\epsilon_3\epsilon_3\epsilon_3}+4\boldsymbol{\Gamma}_{\epsilon_3\epsilon_3\epsilon_2\epsilon_2}\boldsymbol{\Gamma}_{\epsilon_2\epsilon_2\epsilon_3\epsilon_3}\right]^{\frac{1}{2}}}\right]\end{aligned} \tag{II.14}$$

for the two first excited states of interest here. They can be rewritten in the simplest forms as

$$\begin{aligned}\boldsymbol{G}_{\epsilon_2\epsilon_2\epsilon_2\epsilon_2}(t) &= \boldsymbol{\Xi}_{-+}e^{\boldsymbol{\lambda}_+t}+\boldsymbol{\Xi}_{+-}e^{\boldsymbol{\lambda}_-t},\\ \boldsymbol{G}_{\epsilon_3\epsilon_3\epsilon_3\epsilon_3}(t) &= \boldsymbol{\Xi}_{+-}e^{\boldsymbol{\lambda}_+t}+\boldsymbol{\Xi}_{-+}e^{\boldsymbol{\lambda}_-t},\end{aligned} \tag{II.15}$$

where the notations $\boldsymbol{\lambda}_\pm=-\frac{1}{2}(\boldsymbol{\Gamma}_{\epsilon_2\epsilon_2\epsilon_2\epsilon_2}+\boldsymbol{\Gamma}_{\epsilon_3\epsilon_3\epsilon_3\epsilon_3})\pm\frac{1}{2}\boldsymbol{\Delta}$, $\boldsymbol{\Xi}_{-+}=(\boldsymbol{\Delta}-\boldsymbol{\Gamma}_{\epsilon_2\epsilon_2\epsilon_2\epsilon_2}+\boldsymbol{\Gamma}_{\epsilon_3\epsilon_3\epsilon_3\epsilon_3})/2\boldsymbol{\Delta}$, and $\boldsymbol{\Xi}_{+-}=(\boldsymbol{\Delta}+\boldsymbol{\Gamma}_{\epsilon_2\epsilon_2\epsilon_2\epsilon_2}-\boldsymbol{\Gamma}_{\epsilon_3\epsilon_3\epsilon_3\epsilon_3})/2\boldsymbol{\Delta}$ have been introduced conjointly with the additional quantity $\boldsymbol{\Delta}=[\boldsymbol{\Gamma}^2_{\epsilon_2\epsilon_2\epsilon_2\epsilon_2}-2\boldsymbol{\Gamma}_{\epsilon_3\epsilon_3\epsilon_3\epsilon_3}\boldsymbol{\Gamma}_{\epsilon_2\epsilon_2\epsilon_2\epsilon_2}+\boldsymbol{\Gamma}^2_{\epsilon_3\epsilon_3\epsilon_3\epsilon_3}+4\boldsymbol{\Gamma}_{\epsilon_3\epsilon_3\epsilon_2\epsilon_2}\boldsymbol{\Gamma}_{\epsilon_2\epsilon_2\epsilon_3\epsilon_3}]^{\frac{1}{2}}$. Notice that these population evolution Liouvillians are the only ones required for our evaluation because during the course of the 4WM PE process higher excited states are never populated.

III. VIBRATIONAL DYNAMICS UNDERLYING THE 4WM PE SIGNAL FOR ANHARMONIC AND COUPLED OSCILLATORS

To evaluate the vibrational dynamical evolution underlying the 4WM PE signal arising from a molecular system made of two vibrational oscillators undergoing anharmonicity and mode-mode coupling, we use the traditional photon-echo geometry for the three infrared laser beams inducing a coherent signal, the 4WM PE signal, obtained in the direction $-\vec{k}_a+\vec{k}_b+\vec{k}_c$ by heterodyne detection. The interaction Hamiltonian between the molecular system and the laser beams is given by

$$\boldsymbol{V}(t)=-\sum_{p=a,b,c}\mathcal{A}_p(t-T_p)\left[\vec{\boldsymbol{\mu}}\cdot\vec{E}_p\,e^{-i\omega_p t+i\vec{k}_p\cdot\vec{r}}+\text{c.c.}\right], \tag{III.1}$$

where the notation c.c. stands for the complex conjugate part and $\mathcal{A}_p(t-T_p)$ represents the envelop of the pulsed laser field p given by

$$\mathcal{A}_p(t-T_p)=\sqrt{\gamma_p}\exp(-\gamma_p|t-T_p|), \tag{III.2}$$

where T_p and γ_p^{-1} are the probing time and the duration of the pulse, respectively. Here, the laser pulse is described by a double-sided exponential, because this is the only analytical shape which allows a complete analytical evaluation of the polarization. As usual, $\vec{\boldsymbol{\mu}}$ is the dipole moment operator and the quantities ω_p and $\vec{k}_p$ are standard notations for the frequency and the wave vector of the field p, respectively. It is well established that 4WM PE and many other related nonlinear optical processes [31–39] are accounted for by the third-order perturbation term of the density matrix with respect to the laser-molecule interaction $\boldsymbol{V}(t)$ described previously. Then, for the three-pulse process we want to discuss here, the contribution to the third-order term of the density matrix $\boldsymbol{\rho}^{(3)}(t)$ takes the form

$$\begin{aligned}\boldsymbol{\rho}^{(3)}(t) &= \frac{i}{\hbar^3}\int_{t_0}^{t}d\tau_3\int_{t_0}^{\tau_3}d\tau_2\int_{t_0}^{\tau_2}d\tau_1\boldsymbol{G}(t-\tau_3)\boldsymbol{L}_{\text{v}}(\tau_3)\\ &\quad\times\boldsymbol{G}(\tau_3-\tau_2)\boldsymbol{L}_{\text{v}}(\tau_2)\boldsymbol{G}(\tau_2-\tau_1)\boldsymbol{L}_{\text{v}}(\tau_1)\boldsymbol{\rho}(t_0),\end{aligned} \tag{III.3}$$

where the interaction Liouvillian is defined by $\boldsymbol{L}_{\text{v}}(\tau_i)=[\boldsymbol{V}(\tau_i),\ldots]$. The various $\boldsymbol{G}(\tau_i-\tau_j)$ are the free-evolution Liouvillians of the vibrational system alone, corresponding to $\boldsymbol{G}(\tau_i-\tau_j)=e^{-\frac{i}{\hbar}\boldsymbol{L}(\tau_i-\tau_j)}$, where $\boldsymbol{L}=[\boldsymbol{H},\ldots]$ with $\boldsymbol{H}$ being the free-vibrational Hamiltonian. They account for the evolution of the populations $\boldsymbol{G}_{mmmm}(\tau_i-\tau_j)$ given by Eqs. (II.14) and (II.15), as well as for the evolution of the coherences $\boldsymbol{G}_{mnmn}(\tau_i-\tau_j)$ with $m\neq n$. Notice that $\boldsymbol{G}_{mnmn}(\tau_i-\tau_j)$ is

diagonal in the coherence Liouvillian subspace and results in the general form

$$\boldsymbol{G}_{mnmn}(\tau_i-\tau_j)=e^{-i\omega_{mn}(\tau_i-\tau_j)-\boldsymbol{\Gamma}_{mnmn}(\tau_i-\tau_j)}. \quad \text{(III.4)}$$

The various density matrix elements required for the evaluation of the third-order polarization are obtained from the set of pathways contributing to the third-order process. The pathways are listed in the Appendix. Of course, from the diagonalization procedure, the dipole moments in the zeroth-order basis set representation are redistributed among the eigenstates. Some of the components of the dipole moments are orders of magnitude smaller than the other ones. This is particularly the case for the transition dipole moments $\vec{\boldsymbol{\mu}}_{\epsilon_2\epsilon_3}$, $\vec{\boldsymbol{\mu}}_{\epsilon_4\epsilon_5}$, $\vec{\boldsymbol{\mu}}_{\epsilon_5\epsilon_6}$, and $\vec{\boldsymbol{\mu}}_{\epsilon_4\epsilon_6}$. Therefore, their contributions are meaningless and not accounted for here. Of course, according to the geometry of the experiment determined by the phase-matched conditions and the energetic and temporal structures of the laser excitations, not all the pathways and interaction field orderings are considered. Also, in the Appendix, we indicate for each interaction term which component needs to be retained in the framework of the rotating wave approximation (RWA). If we analyze all the possible field orderings with each field interacting only once, it is worth mentioning, assuming RWA, that we have the wave vector combinations $(-,+,+)$, $(+,-,+)$, and $(-,+,+)$. The first field ordering corresponds, for increasing times, to interactions with the field components $-\vec{k}_a \rightarrow +\vec{k}_b \rightarrow +\vec{k}_c$ like in 4WM PE experiments under the impulse limit approximation where no pulse overlap is considered. Now, if the overlap between the pulsed fields b and c has to be accounted for, then we must consider the two field orderings $-\vec{k}_a \rightarrow +\vec{k}_{b(c)} \rightarrow +\vec{k}_{c(b)}$. Besides, if fields a and b overlap, like is the case when we record the signal over the full range of delay times between fields a and b, then other field orderings contribute involving the additional chronological orderings $+\vec{k}_{b(c)} \rightarrow -\vec{k}_a \rightarrow +\vec{k}_{c(b)}$ and $+\vec{k}_{b(c)} \rightarrow +\vec{k}_{c(b)} \rightarrow -\vec{k}_a$. This is typically the case in 2D infrared spectroscopy experiments involving a double Fourier transform over time delay between fields a and b and over real time. Also, because of broad pulse linewidths, a higher number of states have to be included in the dynamics. Notice that for descriptions restricted to two- or three-level systems, this last field combination does not contribute.

The formal expression of the third-order polarization in the phase-matched direction $-\vec{k}_a+\vec{k}_b+\vec{k}_c$, required in 4WM PE experiments, is given by

$$\vec{\boldsymbol{P}}^{(3)}_{-\vec{k}_a+\vec{k}_b+\vec{k}_c}(\vec{r},t)=\sum_{\epsilon_i,\epsilon_j}\boldsymbol{\rho}^{(3)}_{\epsilon_i\epsilon_j}(t)\vec{\boldsymbol{\mu}}_{\epsilon_j\epsilon_i}, \quad \text{(III.5)}$$

where, from Eq. (III.2), the density matrix elements can be written as

$$\begin{aligned}\boldsymbol{\rho}^{(3)}_{\epsilon_i\epsilon_j}(t)=\frac{i}{\hbar^3}\sum_{\{n\}}{}'\sum_{r,q,p}\int_{t_0}^{t}d\tau_3\int_{t_0}^{\tau_3}d\tau_2\int_{t_0}^{\tau_2}d\tau_1\mathcal{A}_r(\tau_1-T_r)\\ \times\mathcal{A}_q(\tau_2-T_q)\mathcal{A}_p(\tau_3-T_p)\\ \times\boldsymbol{R}_{n,\epsilon_i\epsilon_j}(\tau_1,\tau_2,\tau_3,t)e^{-i(\vec{k}_a-\vec{k}_b-\vec{k}_c)\cdot\vec{r}}. \quad \text{(III.6)}\end{aligned}$$

Each n specifies a particular pathway in the Liouvillian space contributing to the density matrix elements. There are 64 different contributions. The symbol $\sum_{r,q,p}$ stands for the summation over the field combinations satisfying the phase-matched direction in the framework of the rotating wave approximation where the only combinations of field components satisfying the secular approximation are retained. In addition, the symbol $\sum'_{\{n\}}$ means that only the values of n associated with the particular density matrix element $\boldsymbol{\rho}^{(3)}_{\epsilon_i\epsilon_j}(t)$ must be retained. Finally, the general mathematical structure of $\boldsymbol{R}_{n,\epsilon_i\epsilon_j}(\tau_1,\tau_2,\tau_3,t)$ is of the type

$$\boldsymbol{R}_{n,\epsilon_i\epsilon_j}(\tau_1,\tau_2,\tau_3,t)=Q_{n,r,q,p}e^{A_{n,r,q,p}\tau_3+B_{n,r,q}\tau_2+C_{n,r}\tau_1}e^{D_{n,r,q,p}t}, \quad \text{(III.7)}$$

where all the amplitudes $Q_{n,r,q,p}$ and exponential arguments $A_{n,r,q,p}$, $B_{n,r,q}$, $C_{n,r}$, and $D_{n,r,q,p}$ can straightforwardly be obtained from identification of relation (III.7) with the various matrix elements of the quantity $\langle\epsilon_i|\boldsymbol{G}(t-\tau_3)\boldsymbol{L}_{\rm v}(\tau_3)\boldsymbol{G}(\tau_3-\tau_2)\boldsymbol{L}_{\rm v}(\tau_2)\boldsymbol{G}(\tau_2-\tau_1)\boldsymbol{L}_{\rm v}(\tau_1)\boldsymbol{\rho}(t_0)|\epsilon_j\rangle$ when expressed in terms of the evolution Liouvillians given by Eqs. (II.15) and (III.13) with the definition of the interaction Liouvillian $\boldsymbol{L}_{{\rm v},ijkl}(\tau)=\boldsymbol{V}_{ik}(\tau)\delta_{lj}-\boldsymbol{V}_{lj}(\tau)\delta_{ik}$.

In a 4WM PE experiment, the phase of the third-order polarization built from successive excitation by the laser pulses contains all the information about the various transition frequencies participating in the process underlying the detected signal. Then, using heterodyne detection by mixing the third-order signal with a local field oscillator $\vec{E}_{\rm lo}(\vec{r},\tau)$ given by

$$\vec{E}_{\rm lo}(\vec{r},\tau)=\mathcal{A}_{\rm lo}(\tau-t)[\vec{E}_{\rm lo}(\omega_{\rm lo})\,e^{-i\omega_{\rm lo}\tau+i\vec{k}_{\rm lo}\cdot\vec{r}+i\Psi}+\text{c.c.}], \quad \text{(III.8)}$$

with adjustable phase Ψ and space and time overlaps, the phase information is preserved, whereas it is lost in homodyne detection. For the sake of simplicity, the envelop of the local oscillator is chosen to be $\mathcal{A}_{\rm lo}(\tau-t)=\delta(\tau-t)$. Therefore, with a convenient choice of having the local field amplitude larger than the signal amplitude, the intensity of the 4WM PE signal associated with the electric field $E_{\rm 4WM\,PE}$ is negligible. Then, substracting the intensity of the local field, we have

$$\begin{aligned}I_{\rm 4WM\,PE}(t)&=I_{\rm tot}(t)-\int_{-\infty}^{\infty}d\tau\,E_{\rm lo}(\vec{r},\tau)^2\\ &\approx 2\int_{-\infty}^{\infty}d\tau\,\vec{E}_{\rm lo}(\vec{r},\tau)\cdot\vec{E}_{\rm 4WM\,PE}(\vec{r},\tau) \quad \text{(III.9)}\end{aligned}$$

or, in terms of the phase-matched component of the corresponding polarization given by Eq. (III.5) and rejecting the high frequency terms, it can be expressed as

$$I_{\rm 4WM\,PE}(t)\approx 4\,\mathrm{Re}\left\{i\,\vec{E}^{\star}_{\rm lo}(\omega_{\rm lo})\cdot\vec{\boldsymbol{P}}^{(3)}_{-\vec{k}_a+\vec{k}_b+\vec{k}_c}(\vec{r},t)\,e^{i\omega_{\rm lo}t-i\vec{k}_{\rm lo}\cdot\vec{r}-i\Psi}\right\}. \quad \text{(III.10)}$$

In addition, with the convenient choices of the wave vector $\vec{k}_{\rm lo}=-\vec{k}_a+\vec{k}_b+\vec{k}_c$ and frequency $\omega_{\rm lo}=-\omega_a+\omega_b+\omega_c$, appropriate to the phase-matched conditions chosen in this

experiment, we get

$$I_{4\mathrm{WM\,PE}}(t) \approx -4\,\mathrm{Im}\left\{\vec{E}^{\star}_{\mathrm{lo}}(\omega_{\mathrm{lo}})\cdot\vec{\boldsymbol{P}}^{(3)}_{-\vec{k}_a+\vec{k}_b+\vec{k}_c}(\vec{r},t)\,e^{i\omega_{\mathrm{lo}}t-i\vec{k}_{\mathrm{lo}}\cdot\vec{r}-i\Psi}\right\}, \tag{III.11}$$

which gives in turn, on account of the expression (III.6), the following result:

$$\begin{aligned} I_{4\mathrm{WM\,PE}}(t) \approx -\frac{4}{\hbar^3}\,\mathrm{Re}\Bigg\{ & \vec{E}^{\star}_{\mathrm{lo}}(\omega_{\mathrm{lo}})\cdot\vec{\boldsymbol{\mu}}_{\epsilon_j\epsilon_i}e^{i\omega_{\mathrm{lo}}t-i\Psi}\sum_{\epsilon_i\epsilon_j} \\ & \times \sum_{\substack{r,q,p \\ \vec{k}_r+\vec{k}_q+\vec{k}_p=-\vec{k}_a+\vec{k}_b+\vec{k}_c}} \int_{t_0}^{t} d\tau_3 \int_{t_0}^{\tau_3} d\tau_2 \int_{t_0}^{\tau_2} d\tau_1 \\ & \times \mathcal{A}_r(\tau_1-T_r)\mathcal{A}_q(\tau_2-T_q)\mathcal{A}_p(\tau_3-T_p) \\ & \times \boldsymbol{R}_{n,\epsilon_i\epsilon_j}(\tau_1,\tau_2,\tau_3,t)\Bigg\}. \end{aligned} \tag{III.12}$$

Assuming the dipole moments as well as the amplitude of the local oscillator $\vec{E}^{\star}_{\mathrm{lo}}(\omega_{\mathrm{lo}})$ real, by an appropriate choice of the local oscillator phase Ψ, we can test the real and the imaginary parts of the polarization by taking advantage of the heterodyne detection. For instance, with $\Psi=0$ or $\Psi=\Pi/2$, we get the 4WM PE signal into the form

$$\begin{aligned} I_{4\mathrm{WM\,PE}}(t) \approx -\frac{4}{\hbar^3}\sum_{\epsilon_i\epsilon_j}\vec{E}_{\mathrm{lo}}(\omega_{\mathrm{lo}})\cdot\vec{\boldsymbol{\mu}}_{\epsilon_j\epsilon_i}\begin{Bmatrix}\mathrm{Re}_{\mathrm{if}\ \Psi=0}\\ \mathrm{Im}_{\mathrm{if}\ \Psi=\pi/2}\end{Bmatrix} \\ \times\Bigg\{ e^{i\omega_{\mathrm{lo}}t}\sum_{\substack{r,q,p \\ \vec{k}_r+\vec{k}_q+\vec{k}_p=-\vec{k}_a+\vec{k}_b+\vec{k}_c}} \int_{t_0}^{t} d\tau_3 \int_{t_0}^{\tau_3} d\tau_2 \int_{t_0}^{\tau_2} d\tau_1 \\ \times \mathcal{A}_r(\tau_1-T_r)\mathcal{A}_q(\tau_2-T_q)\mathcal{A}_p(\tau_3-T_p) \\ \times \boldsymbol{R}_{n,\epsilon_i\epsilon_j}(\tau_1,\tau_2,\tau_3,t)\Bigg\}, \end{aligned} \tag{III.13}$$

meaning that the real part Re or the imaginary part Im of the second set of curly brackets has to be taken for the value $\Psi=0$ or $\Psi=\pi/2$, respectively. This last expression (III.13) is used in the next section to perform time-dependent simulations on the detected signal to analyze the role played simultaneously by the anharmonicity and the mode-mode coupling, on account of the redistribution of the relaxation, dephasing, and transition constants. Notice that for the sake of simplicity, the triple time integrations are not explicitly introduced. Once the evaluation of the various constants in expression (III.7) are obtained from identification as previously mentioned, the required time integration of the general type of terms

$$\begin{aligned} \int_{t_0}^{t} d\tau_3 \int_{t_0}^{\tau_3} d\tau_2 \int_{t_0}^{\tau_2} d\tau_1 \mathcal{A}_r(\tau_1-T_r)\mathcal{A}_q(\tau_2-T_q) \\ \times \mathcal{A}_p(\tau_3-T_p)\,e^{A_{n,r,q,p}\tau_3+B_{n,r,q}\tau_2+C_{n,r}\tau_1} \end{aligned} \tag{III.14}$$

can be straightforwardly done.

IV. NUMERICAL SIMULATIONS AND DISCUSSIONS

This section is devoted to a number of numerical simulations to emphasize the role the anharmonicity as well as the role the mode-mode couplings plays in the two-mode model. To analyze the internal vibrational dynamics induced by the laser beams in the present model, we apply the more informative heterodyne detection by introducing a local oscillator. The phase of the third-order polarization induced in the $-\vec{k}_a+\vec{k}_b+\vec{k}_c$ phase-matched photon-echo geometry can be tested and appears to be very sensitive to the type and the magnitude of the internal couplings. These simulations will be very useful to illustrate the 4WM PE signal evaluated analytically in the former sections.

Throughout, since we are dealing with heterodyne detection, we consider two different situations where the phase of the local field oscillator respectively corresponds to $\Psi=0$ and $\Psi=\pi/2$. They enable us to test separately the real and the imaginary part of the third-order polarization, for different types of coupling and for the off-resonance parameters between the excitation laser beam chosen to be the same for the three beams and the first transition $|00\rangle\rightarrow|10\rangle$. First, the probing times of the laser pulses are $T_a=-0.7c^{-1}$ ps, $T_b=0$ ps, and $T_c=c^{-1}$ ps, where c stands for the speed of light expressed in cm/ps. The bandwidths of the laser pulses are all the same, that is $\gamma_i=30\ \mathrm{cm}^{-1}$ for all i. Similarly, the laser frequencies are chosen to be identical so that $\omega_p=2015\ \mathrm{cm}^{-1}$ for all p. In addition, for a vibrational mode, the transition dipole moments are assumed to satisfy harmonic scaling law [25,26], so the dipole matrix elements associated with two sequential excitations are related, for the fundamental and overtone transitions, by the expressions $\langle 01|\vec{\boldsymbol{\mu}}|02\rangle=\sqrt{2}\langle 00|\vec{\boldsymbol{\mu}}|01\rangle$ and $\langle 10|\vec{\boldsymbol{\mu}}|20\rangle=\sqrt{2}\langle 00|\vec{\boldsymbol{\mu}}|10\rangle$. Also, we assume the dipole moments to be real with the following values $\mu_{12}=\mu_{35}=1$, $\mu_{13}=\mu_{25}=1.2$, $\mu_{24}=\sqrt{2}$, and $\mu_{36}=\mu_{25}=1.2\sqrt{2}$. All the other dipole moments equal zero. Notice that an analogous scaling law can be found for the vibrational population and phase relaxations [40,41]. The frequencies of the vibrational harmonic modes are $\omega_1=2015\ \mathrm{cm}^{-1}$ and $\omega_2=2084\ \mathrm{cm}^{-1}$. Finally, we list the values of the relaxation and dephasing constants in terms of the three parameters $a=8\ \mathrm{cm}^{-1}$, $b=10\ \mathrm{cm}^{-1}$, and $c=2\ \mathrm{cm}^{-1}$. We have for the relaxation constants $\Gamma_{1111}=0$, $\Gamma_{2222}=a$, $\Gamma_{3333}=b$, $\Gamma_{4444}=2a$, $\Gamma_{5555}=a+b$, and $\Gamma_{66666}=2b$. With the pure dephasing constant c assumed to be identical for all the states, all the Γ_{ijij} are readily obtained. Moreover, we require the transition constants satisfying the summation rule $\Gamma_{jjjj}=-\sum_{i\neq j}\Gamma_{iijj}$. We get $\Gamma_{11nn}=-\Gamma_{nnnn}$ if $n=1$ and 2, $\Gamma_{2244}=\Gamma_{3355}=\Gamma_{1122}$, $\Gamma_{2255}=\Gamma_{3366}=\Gamma_{1133}$, $\Gamma_{1144}=-\Gamma_{4444}-\Gamma_{2244}$, $\Gamma_{1155}=-\Gamma_{5555}-\Gamma_{2255}-\Gamma_{3355}$, and finally $\Gamma_{1166}=-\Gamma_{6666}-\Gamma_{3366}$. As previously mentioned, all the other relaxation, dephasing and transition constants are zero. With these physical parameters, the numerical simulations can readily be performed. Notice that all the time dependences simulated here are represented in arbitrary units. However, their relative magnitudes are exact because the same multiplicative constant has been used all along. This means that the vertical scale is the same for all the figures. Also, we have to bear in mind that all the simulations represent the variations of $I_{4\mathrm{WM\,PE}}(t)$ where the intensity of the local field has been subtracted.

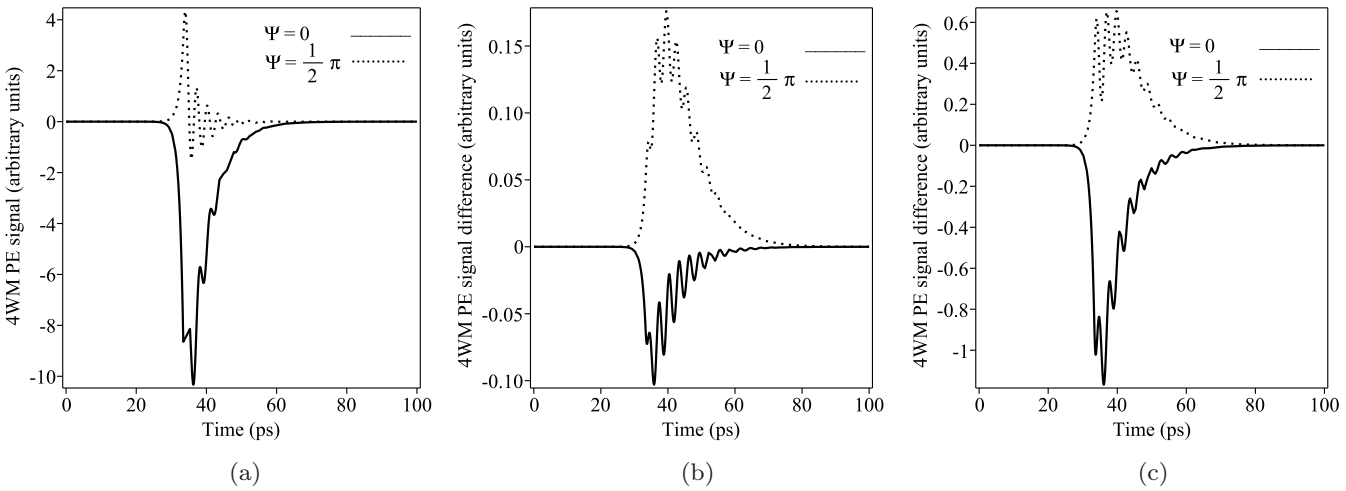

FIG. 2. Time dependence of the 4WM PE signal for two different phases of the local oscillator. Three different sets of anharmonic couplings u_{111} and u_{222} are considered: (a) $u_{111} = 1\ \text{cm}^{-1}$, $u_{222} = 1\ \text{cm}^{-1}$; (b) $u_{111} = 15\ \text{cm}^{-1}$, $u_{222} = 15\ \text{cm}^{-1}$; and (c) $u_{111} = 30\ \text{cm}^{-1}$, $u_{222} = 30\ \text{cm}^{-1}$. All the other mode-mode coupling parameters are zero: $u_{12} = u_{112} = u_{122} = 0$. The laser field frequencies are $\omega_a = \omega_b = \omega_c = 2015\ \text{cm}^{-1}$.

We first start with the time dependence of the 4WM PE signal obtained by heterodyne detection using two different phases. The two particular choices, say $\Psi = 0$ and $\Psi = \pi/2$ for the local field oscillator, as indicated in Fig. 2, enable us to test the real and imaginary parts of the third-order polarization, respectively. To be more illustrative, Fig. 2 shows the time dependence of the 4WM PE signal with negligible anharmonicity where, as usual, the intensity of the local field has been subtracted. Figures 2(b) and 2(c) correspond to different sets of anharmonic parameters u_{111} and u_{222}, as indicated in the caption. Notice that in these two last figures obtained for increasing values of the anharmonic parameters, we drew the differences of the 4WM PE signal with respect to the one obtained in Fig. 1(a). From the real and imaginary parts, we can follow the phase of the polarization. The 4WM PE signal decays with the values of the dephasing constants associated with the states contributing to the various pathways. Of course, in our simulation, since we chose the laser fields resonant with the harmonic oscillator 1, the dominant contribution evolves with the dephasing constant of level $|10\rangle$. The oscillations clearly state that even for pulse linewidths of 30 cm^{-1}, that is, of the order of 1 ps, oscillator 2 comes into play and we have contributions to the 4WM PE signal where coherence is created simultaneously in both vibrational modes. Next, in Fig. 3, the same type of variations are represented for the different sets of mode-mode coupling parameters given in the figure caption. Of course, here, due to the couplings between states associated with different oscillators, more combinations appear, giving rise to additional pathways. Therefore, as we can see from Fig. 3, for weak mode-mode couplings we recover the same type of oscillating behavior corresponding to pathways involving excited states of different oscillators. In addition to these contributions, we see by increasing the magnitude of the mode-mode couplings that additional oscillating terms contribute with different frequencies. Of course, because of the large number of pathways participating in the third-order

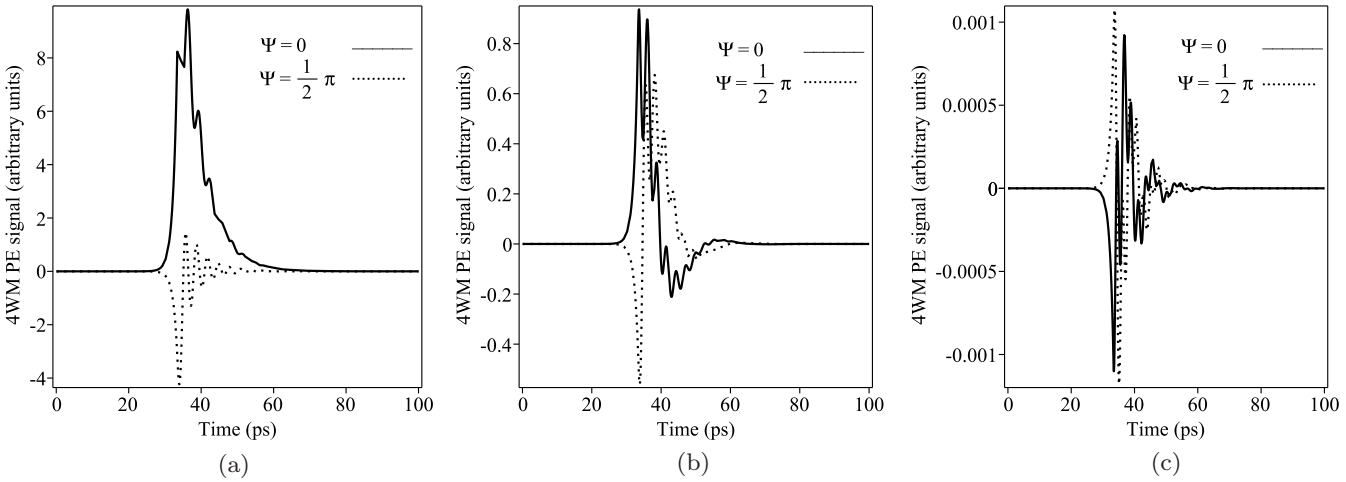

FIG. 3. Time dependence of the 4WM PE signal for two different phases of the local oscillator. Three different sets of mode-mode couplings u_{12}, u_{112}, and u_{122} are considered: (a) $u_{12} = 1\ \text{cm}^{-1}$, $u_{112} = 1\ \text{cm}^{-1}$, $u_{122} = 1\ \text{cm}^{-1}$; (b) $u_{12} = 25\ \text{cm}^{-1}$, $u_{112} = 15\ \text{cm}^{-1}$, $u_{122} = 15\ \text{cm}^{-1}$; and (c) $u_{12} = 50\ \text{cm}^{-1}$, $u_{112} = 30\ \text{cm}^{-1}$, $u_{122} = 30\ \text{cm}^{-1}$. All the other anharmonic coupling parameters are zero: $u_{111} = u_{222} = 0$. The laser field frequencies are $\omega_a = \omega_b = \omega_c = 2015\ \text{cm}^{-1}$.

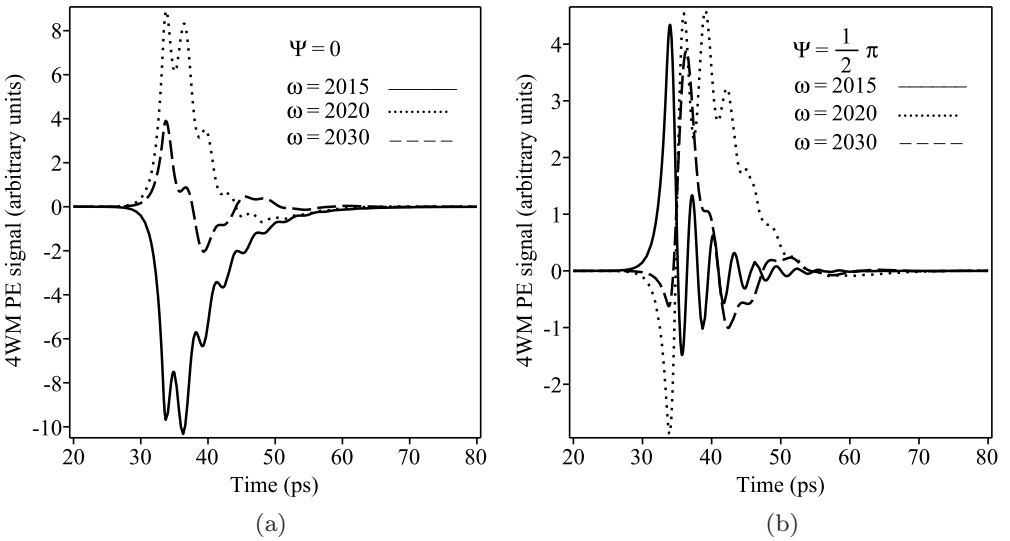

FIG. 4. Time dependence of the 4WM PE signal for three different laser field frequencies. The cases of two different local oscillator phases, (a) $\Psi = 0$ and (b) $\Psi = \pi/2$, are considered. The anharmonic couplings are $u_{111} = 1$ cm^{-1}, $u_{222} = 1$ cm^{-1}, and all the other mode-mode coupling parameters are zero: $u_{12} = u_{112} = u_{122} = 0$.

polarization, it is not easy to single out a specific contribution even if it is clear, as are the cases in Figs. 3(b) and 3(c), that at least two different frequencies modulate the 4WM PE signal.

Finally, we come to the role played by the off-resonance parameter. In the last set of figures, we discuss the influence of the off-resonance parameter between the laser field and harmonic oscillator 1. Here, because of the nonresonant excitation conditions and frequency shifts induced by anharmonicity and mode-mode coupling, a larger number of different pathways contribute efficiently, making the interpretation quite tedious. The problem is still more complicated for laser excitations with different frequencies. This type of experimental condition can sometimes be of interest to analyze some specific processes.

In our simulations, all laser field frequencies are chosen to be identical. Here, we can distinguish two different effects according to the respective values of the transition frequency changes induced by the interaction terms. In the simplest case, starting from a resonant situation, as chosen initially for our simulations, and shifting the laser field frequency, the overlap between the vibrational resonance and the laser spectral distribution decreases and there is a global decrease of the 4WM PE signal. In this case, the general structure of the time dependence is not altered. This is true until the change of the laser frequency notably modifies the balance of the contributions associated with the different pathways. In this case, the time dependence will reflect the physical characteristics of the processes selected by the laser excitation structure. In Figs. 4 and 5 we exhibit, as previously, the time dependence of 4WM PE signal for three different laser field frequencies and two different local oscillator phases as indicated in the figures. Figures 4 and 5 differ by the choice of the anharmonic parameters. In all the figures, we clearly

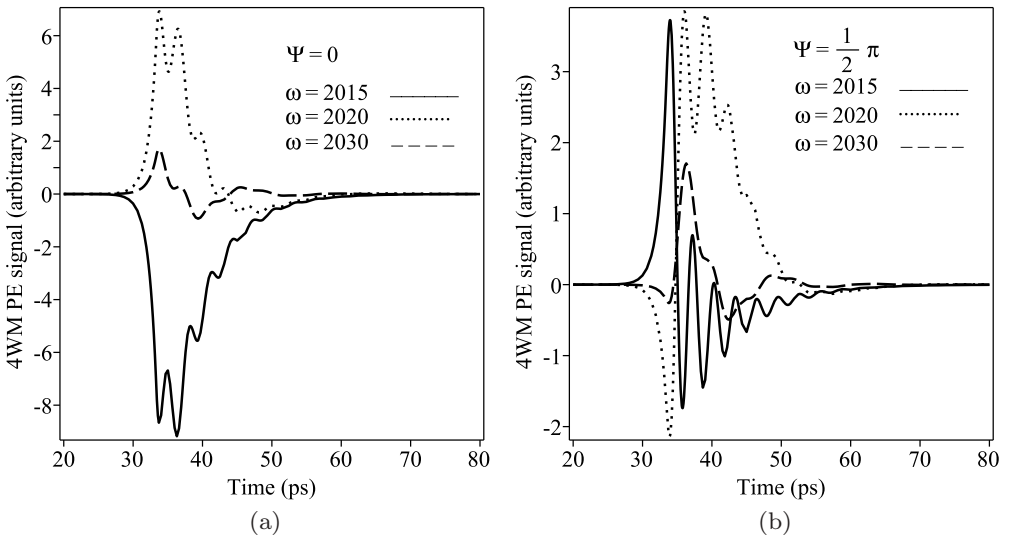

FIG. 5. We show the same variations as in Fig. 4 for a different set of anharmonic couplings given by $u_{111} = 30$ cm^{-1}, $u_{222} = 30$ cm^{-1}. Like previously, all the other mode-mode coupling parameters are zero: $u_{12} = u_{112} = u_{122} = 0$.

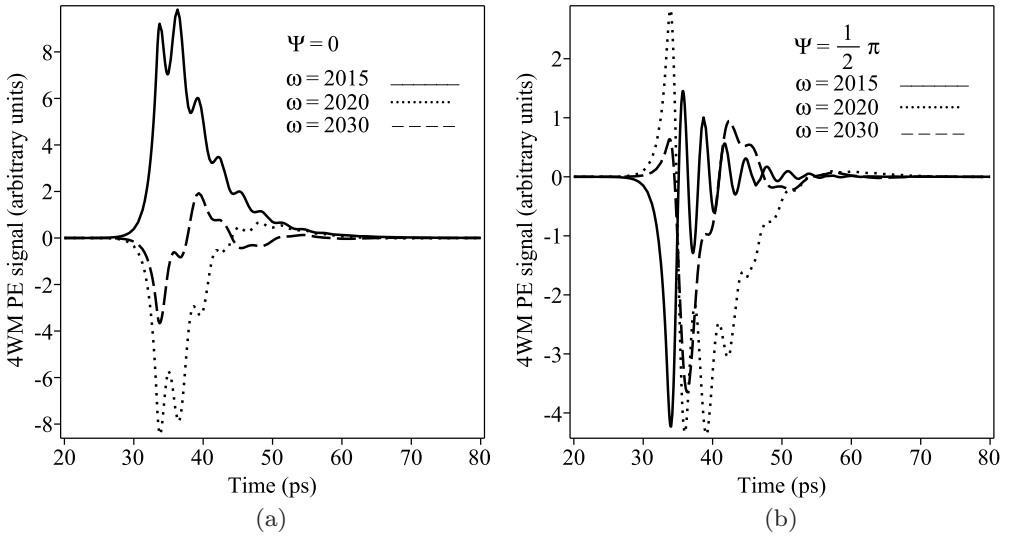

FIG. 6. Time dependence of the 4WM photon-echo signal for three different laser field frequencies. The case of two different local oscillator phases (a) $\Psi = 0$ and (b) $\Psi = \pi/2$, are considered. The mode-mode couplings are $u_{12} = 1\ \mathrm{cm}^{-1}$, $u_{112} = 1\ \mathrm{cm}^{-1}$, $u_{122} = 1\ \mathrm{cm}^{-1}$, and all the other anharmonic coupling parameters are zero: $u_{111} = u_{222} = 0$.

see that, for the largest value of the off-resonance parameter, a second frequency of 30 cm^{-1} comes into play.

The same type of variations are represented in Figs. 6 and 7 for the mode-mode coupling case. Of course, here, because the energy shifts are more important, the contribution obtained when the laser frequency is resonant with the unperturbed harmonic oscillator frequency at 2015 cm^{-1} is no longer dominant. It is really when the off-resonance parameter compensates for the energy shift that we get the bigger 4WM PE response.

V. CONCLUSION

In this work, we have developed a detailed description of the dynamics underlying a three-pulse 4WM PE process performed on a vibronic system made of two coupled vibrational modes. For weak intermode coupling, the perturbation mainly opens new pathways which contribute to the 4WM PE signal, but basically the internal dynamics of the vibrational systems remains the same, because the physical constants are not altered by the perturbation. For larger values of anharmonicity and intermode coupling, this is no longer the case and a complete redistribution of the relaxation and dephasing constants has to be considered. Also, since the effect of finite laser pulse linewidths is always important in short time experiments, the possibility of different chronologically ordered interactions has to be accounted for. By a complete diagonalization of the anharmonic and mode-mode coupling terms and an analytical description of the laser pulses, we have evaluated analytically the 4WM PE signal. The particular roles of anharmonicity and mode-mode coupling have been discussed separately. Also, the signal shows a high sensitivity

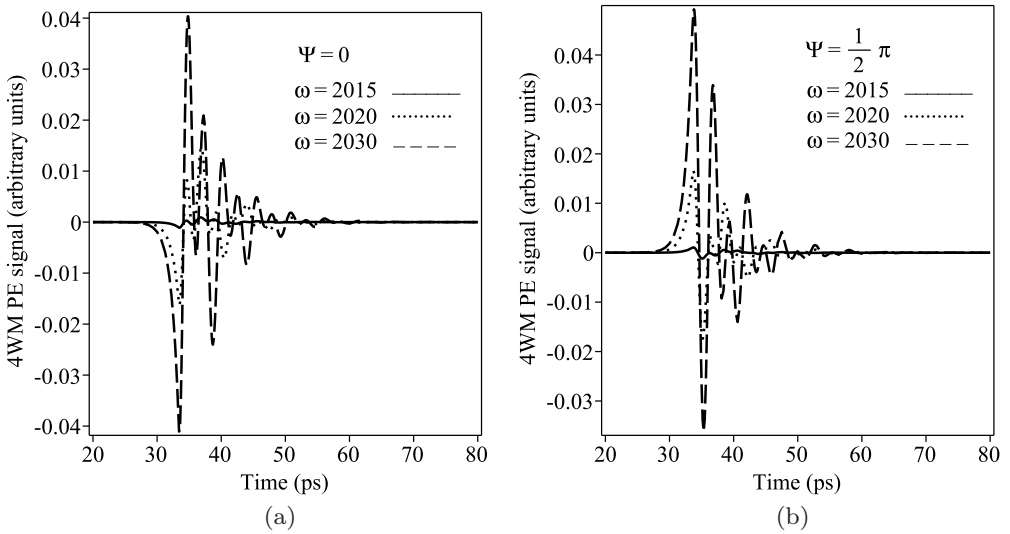

FIG. 7. We show the same variations as in Fig. 6 for a different set of mode-mode couplings given by $u_{12} = 30\ \mathrm{cm}^{-1}$, $u_{112} = 30\ \mathrm{cm}^{-1}$, and $u_{122} = 30\ \mathrm{cm}^{-1}$. Like previously, all the other anharmonic coupling parameters are zero: $u_{111} = u_{222} = 0$.

to the internal structure and experimental conditions, as is frequently the case in nonlinear optical spectroscopy.

ACKNOWLEDGMENTS

This work was supported by the Academia Sinica and by the National Science Council of Taiwan (Grant No. 96-2113-M001-025-MY2).

APPENDIX

We describe all the pathways associated with processes participating in the third-order polarization in the phase-matched direction $-\vec{k}_a + \vec{k}_b + \vec{k}_c$ corresponding to the photon-echo process in Table I. All these pathways are described in the eigenstate basis set $\{|\epsilon_i\rangle\}$. Some pathways whose contributions are meaningless have been omitted as indicated in the caption to Table I.

TABLE I. Pathways participating in the 2D vibrational spectrum. Here, processes associated with dipolar couplings between states $\{|\epsilon_i\rangle \leftrightarrow |\epsilon_j\rangle\}$ for $(i,j) = (2,3)$, (4,5), (5,6), and (4,6) are rejected because the magnitude of their dipole moments are orders of magnitude smaller than the other ones. Also, the symbols $(\pm)$ indicate the signs of the $\vec{k}$ component of the fields which need be considered for the laser field component when the rotating wave approximation is introduced.

$\boldsymbol{\rho}(t)$	$\boldsymbol{G}(t-\tau_3)$	$\boldsymbol{L}_{v[p]}(\tau_3)$	$\boldsymbol{G}(\tau_3-\tau_2)$	$\boldsymbol{L}_{v[q]}(\tau_2)$	$\boldsymbol{G}(\tau_2-\tau_1)$	$\boldsymbol{L}_{v[r]}(\tau_1)$	$\boldsymbol{\rho}(t_0)$
$\epsilon_2\epsilon_1$	$\epsilon_2\epsilon_1\epsilon_2\epsilon_1$	$\epsilon_2\epsilon_1\epsilon_1\epsilon_1^{(+)}$	$\epsilon_1\epsilon_1\epsilon_1\epsilon_1$	$\epsilon_1\epsilon_1\epsilon_1\epsilon_2^{(+)}$	$\epsilon_1\epsilon_2\epsilon_1\epsilon_2$	$\epsilon_1\epsilon_2\epsilon_1\epsilon_1^{(-)}$	$\epsilon_1\epsilon_1$
$\epsilon_3\epsilon_1$	$\epsilon_3\epsilon_1\epsilon_3\epsilon_1$	$\epsilon_3\epsilon_1\epsilon_1\epsilon_1^{(+)}$	$\epsilon_1\epsilon_1\epsilon_1\epsilon_1$	$\epsilon_1\epsilon_1\epsilon_1\epsilon_2^{(+)}$	$\epsilon_1\epsilon_2\epsilon_1\epsilon_2$	$\epsilon_1\epsilon_2\epsilon_1\epsilon_1^{(-)}$	$\epsilon_1\epsilon_1$
$\epsilon_2\epsilon_1$	$\epsilon_2\epsilon_1\epsilon_2\epsilon_1$	$\epsilon_2\epsilon_1\epsilon_2\epsilon_2^{(+)}$	$\epsilon_2\epsilon_2\epsilon_2\epsilon_2$	$\epsilon_2\epsilon_2\epsilon_1\epsilon_2^{(+)}$	$\epsilon_1\epsilon_2\epsilon_1\epsilon_2$	$\epsilon_1\epsilon_2\epsilon_1\epsilon_1^{(-)}$	$\epsilon_1\epsilon_1$
$\epsilon_4\epsilon_2$	$\epsilon_4\epsilon_2\epsilon_4\epsilon_2$	$\epsilon_4\epsilon_2\epsilon_2\epsilon_2^{(+)}$	$\epsilon_2\epsilon_2\epsilon_2\epsilon_2$	$\epsilon_2\epsilon_2\epsilon_1\epsilon_2^{(+)}$	$\epsilon_1\epsilon_2\epsilon_1\epsilon_2$	$\epsilon_1\epsilon_2\epsilon_1\epsilon_1^{(-)}$	$\epsilon_1\epsilon_1$
$\epsilon_5\epsilon_2$	$\epsilon_5\epsilon_2\epsilon_5\epsilon_2$	$\epsilon_5\epsilon_2\epsilon_2\epsilon_2^{(+)}$	$\epsilon_2\epsilon_2\epsilon_2\epsilon_2$	$\epsilon_2\epsilon_2\epsilon_1\epsilon_2^{(+)}$	$\epsilon_1\epsilon_2\epsilon_1\epsilon_2$	$\epsilon_1\epsilon_2\epsilon_1\epsilon_1^{(-)}$	$\epsilon_1\epsilon_1$
$\epsilon_6\epsilon_2$	$\epsilon_6\epsilon_2\epsilon_6\epsilon_2$	$\epsilon_6\epsilon_2\epsilon_2\epsilon_2^{(+)}$	$\epsilon_2\epsilon_2\epsilon_2\epsilon_2$	$\epsilon_2\epsilon_2\epsilon_1\epsilon_2^{(+)}$	$\epsilon_1\epsilon_2\epsilon_1\epsilon_2$	$\epsilon_1\epsilon_2\epsilon_1\epsilon_1^{(-)}$	$\epsilon_1\epsilon_1$
$\epsilon_3\epsilon_1$	$\epsilon_3\epsilon_1\epsilon_3\epsilon_1$	$\epsilon_3\epsilon_1\epsilon_3\epsilon_2^{(+)}$	$\epsilon_3\epsilon_2\epsilon_3\epsilon_2$	$\epsilon_3\epsilon_2\epsilon_1\epsilon_2^{(+)}$	$\epsilon_1\epsilon_2\epsilon_1\epsilon_2$	$\epsilon_1\epsilon_2\epsilon_1\epsilon_1^{(-)}$	$\epsilon_1\epsilon_1$
$\epsilon_4\epsilon_2$	$\epsilon_4\epsilon_2\epsilon_4\epsilon_2$	$\epsilon_4\epsilon_2\epsilon_3\epsilon_2^{(+)}$	$\epsilon_3\epsilon_2\epsilon_3\epsilon_2$	$\epsilon_3\epsilon_2\epsilon_1\epsilon_2^{(+)}$	$\epsilon_1\epsilon_2\epsilon_1\epsilon_2$	$\epsilon_1\epsilon_2\epsilon_1\epsilon_1^{(-)}$	$\epsilon_1\epsilon_1$
$\epsilon_5\epsilon_2$	$\epsilon_5\epsilon_2\epsilon_5\epsilon_2$	$\epsilon_5\epsilon_2\epsilon_3\epsilon_2^{(+)}$	$\epsilon_3\epsilon_2\epsilon_3\epsilon_2$	$\epsilon_3\epsilon_2\epsilon_1\epsilon_2^{(+)}$	$\epsilon_1\epsilon_2\epsilon_1\epsilon_2$	$\epsilon_1\epsilon_2\epsilon_1\epsilon_1^{(-)}$	$\epsilon_1\epsilon_1$
$\epsilon_6\epsilon_2$	$\epsilon_6\epsilon_2\epsilon_6\epsilon_2$	$\epsilon_6\epsilon_2\epsilon_3\epsilon_2^{(+)}$	$\epsilon_3\epsilon_2\epsilon_3\epsilon_2$	$\epsilon_3\epsilon_2\epsilon_1\epsilon_2^{(+)}$	$\epsilon_1\epsilon_2\epsilon_1\epsilon_2$	$\epsilon_1\epsilon_2\epsilon_1\epsilon_1^{(-)}$	$\epsilon_1\epsilon_1$
$\epsilon_2\epsilon_1$	$\epsilon_2\epsilon_1\epsilon_2\epsilon_1$	$\epsilon_2\epsilon_1\epsilon_1\epsilon_1^{(+)}$	$\epsilon_1\epsilon_1\epsilon_1\epsilon_1$	$\epsilon_1\epsilon_1\epsilon_1\epsilon_3^{(+)}$	$\epsilon_1\epsilon_3\epsilon_1\epsilon_3$	$\epsilon_1\epsilon_3\epsilon_1\epsilon_1^{(-)}$	$\epsilon_1\epsilon_1$
$\epsilon_3\epsilon_1$	$\epsilon_3\epsilon_1\epsilon_3\epsilon_1$	$\epsilon_3\epsilon_1\epsilon_1\epsilon_1^{(+)}$	$\epsilon_1\epsilon_1\epsilon_1\epsilon_1$	$\epsilon_1\epsilon_1\epsilon_1\epsilon_3^{(+)}$	$\epsilon_1\epsilon_3\epsilon_1\epsilon_3$	$\epsilon_1\epsilon_3\epsilon_1\epsilon_1^{(-)}$	$\epsilon_1\epsilon_1$
$\epsilon_3\epsilon_1$	$\epsilon_3\epsilon_1\epsilon_3\epsilon_1$	$\epsilon_3\epsilon_1\epsilon_3\epsilon_3^{(+)}$	$\epsilon_3\epsilon_3\epsilon_3\epsilon_3$	$\epsilon_3\epsilon_3\epsilon_1\epsilon_3^{(+)}$	$\epsilon_1\epsilon_3\epsilon_1\epsilon_3$	$\epsilon_1\epsilon_3\epsilon_1\epsilon_1^{(-)}$	$\epsilon_1\epsilon_1$
$\epsilon_4\epsilon_3$	$\epsilon_4\epsilon_3\epsilon_4\epsilon_3$	$\epsilon_4\epsilon_3\epsilon_3\epsilon_3^{(+)}$	$\epsilon_3\epsilon_3\epsilon_3\epsilon_3$	$\epsilon_3\epsilon_3\epsilon_1\epsilon_3^{(+)}$	$\epsilon_1\epsilon_3\epsilon_1\epsilon_3$	$\epsilon_1\epsilon_3\epsilon_1\epsilon_1^{(-)}$	$\epsilon_1\epsilon_1$
$\epsilon_5\epsilon_3$	$\epsilon_5\epsilon_3\epsilon_5\epsilon_3$	$\epsilon_5\epsilon_3\epsilon_3\epsilon_3^{(+)}$	$\epsilon_3\epsilon_3\epsilon_3\epsilon_3$	$\epsilon_3\epsilon_3\epsilon_1\epsilon_3^{(+)}$	$\epsilon_1\epsilon_3\epsilon_1\epsilon_3$	$\epsilon_1\epsilon_3\epsilon_1\epsilon_1^{(-)}$	$\epsilon_1\epsilon_1$
$\epsilon_6\epsilon_3$	$\epsilon_6\epsilon_3\epsilon_6\epsilon_3$	$\epsilon_6\epsilon_3\epsilon_3\epsilon_3^{(+)}$	$\epsilon_3\epsilon_3\epsilon_3\epsilon_3$	$\epsilon_3\epsilon_3\epsilon_1\epsilon_3^{(+)}$	$\epsilon_1\epsilon_3\epsilon_1\epsilon_3$	$\epsilon_1\epsilon_3\epsilon_1\epsilon_1^{(-)}$	$\epsilon_1\epsilon_1$
$\epsilon_2\epsilon_1$	$\epsilon_2\epsilon_1\epsilon_2\epsilon_1$	$\epsilon_2\epsilon_1\epsilon_2\epsilon_3^{(+)}$	$\epsilon_2\epsilon_3\epsilon_2\epsilon_3$	$\epsilon_2\epsilon_3\epsilon_1\epsilon_3^{(+)}$	$\epsilon_1\epsilon_3\epsilon_1\epsilon_3$	$\epsilon_1\epsilon_3\epsilon_1\epsilon_1^{(-)}$	$\epsilon_1\epsilon_1$
$\epsilon_4\epsilon_3$	$\epsilon_4\epsilon_3\epsilon_4\epsilon_3$	$\epsilon_4\epsilon_3\epsilon_2\epsilon_3^{(+)}$	$\epsilon_2\epsilon_3\epsilon_2\epsilon_3$	$\epsilon_2\epsilon_3\epsilon_1\epsilon_3^{(+)}$	$\epsilon_1\epsilon_3\epsilon_1\epsilon_3$	$\epsilon_1\epsilon_3\epsilon_1\epsilon_1^{(-)}$	$\epsilon_1\epsilon_1$
$\epsilon_5\epsilon_3$	$\epsilon_5\epsilon_3\epsilon_5\epsilon_3$	$\epsilon_5\epsilon_3\epsilon_2\epsilon_3^{(+)}$	$\epsilon_2\epsilon_3\epsilon_2\epsilon_3$	$\epsilon_2\epsilon_3\epsilon_1\epsilon_3^{(+)}$	$\epsilon_1\epsilon_3\epsilon_1\epsilon_3$	$\epsilon_1\epsilon_3\epsilon_1\epsilon_1^{(-)}$	$\epsilon_1\epsilon_1$
$\epsilon_6\epsilon_3$	$\epsilon_6\epsilon_3\epsilon_6\epsilon_3$	$\epsilon_6\epsilon_3\epsilon_2\epsilon_3^{(+)}$	$\epsilon_2\epsilon_3\epsilon_2\epsilon_3$	$\epsilon_2\epsilon_3\epsilon_1\epsilon_3^{(+)}$	$\epsilon_1\epsilon_3\epsilon_1\epsilon_3$	$\epsilon_1\epsilon_3\epsilon_1\epsilon_1^{(-)}$	$\epsilon_1\epsilon_1$
$\epsilon_2\epsilon_1$	$\epsilon_2\epsilon_1\epsilon_2\epsilon_1$	$\epsilon_2\epsilon_1\epsilon_1\epsilon_1^{(+)}$	$\epsilon_1\epsilon_1\epsilon_1\epsilon_1$	$\epsilon_1\epsilon_1\epsilon_2\epsilon_1^{(-)}$	$\epsilon_2\epsilon_1\epsilon_2\epsilon_1$	$\epsilon_2\epsilon_1\epsilon_1\epsilon_1^{(+)}$	$\epsilon_1\epsilon_1$
$\epsilon_3\epsilon_1$	$\epsilon_3\epsilon_1\epsilon_3\epsilon_1$	$\epsilon_3\epsilon_1\epsilon_1\epsilon_1^{(+)}$	$\epsilon_1\epsilon_1\epsilon_1\epsilon_1$	$\epsilon_1\epsilon_1\epsilon_2\epsilon_1^{(-)}$	$\epsilon_2\epsilon_1\epsilon_2\epsilon_1$	$\epsilon_2\epsilon_1\epsilon_1\epsilon_1^{(+)}$	$\epsilon_1\epsilon_1$
$\epsilon_2\epsilon_1$	$\epsilon_2\epsilon_1\epsilon_2\epsilon_1$	$\epsilon_2\epsilon_1\epsilon_2\epsilon_2^{(+)}$	$\epsilon_2\epsilon_2\epsilon_2\epsilon_2$	$\epsilon_2\epsilon_2\epsilon_2\epsilon_1^{(-)}$	$\epsilon_2\epsilon_1\epsilon_2\epsilon_1$	$\epsilon_2\epsilon_1\epsilon_1\epsilon_1^{(+)}$	$\epsilon_1\epsilon_1$
$\epsilon_4\epsilon_2$	$\epsilon_4\epsilon_2\epsilon_4\epsilon_2$	$\epsilon_4\epsilon_2\epsilon_2\epsilon_2^{(+)}$	$\epsilon_2\epsilon_2\epsilon_2\epsilon_2$	$\epsilon_2\epsilon_2\epsilon_2\epsilon_1^{(-)}$	$\epsilon_2\epsilon_1\epsilon_2\epsilon_1$	$\epsilon_2\epsilon_1\epsilon_1\epsilon_1^{(+)}$	$\epsilon_1\epsilon_1$
$\epsilon_5\epsilon_2$	$\epsilon_5\epsilon_2\epsilon_5\epsilon_2$	$\epsilon_5\epsilon_2\epsilon_2\epsilon_2^{(+)}$	$\epsilon_2\epsilon_2\epsilon_2\epsilon_2$	$\epsilon_2\epsilon_2\epsilon_2\epsilon_1^{(-)}$	$\epsilon_2\epsilon_1\epsilon_2\epsilon_1$	$\epsilon_2\epsilon_1\epsilon_1\epsilon_1^{(+)}$	$\epsilon_1\epsilon_1$
$\epsilon_6\epsilon_2$	$\epsilon_6\epsilon_2\epsilon_6\epsilon_2$	$\epsilon_6\epsilon_2\epsilon_2\epsilon_2^{(+)}$	$\epsilon_2\epsilon_2\epsilon_2\epsilon_2$	$\epsilon_2\epsilon_2\epsilon_2\epsilon_1^{(-)}$	$\epsilon_2\epsilon_1\epsilon_2\epsilon_1$	$\epsilon_2\epsilon_1\epsilon_1\epsilon_1^{(+)}$	$\epsilon_1\epsilon_1$
$\epsilon_2\epsilon_1$	$\epsilon_2\epsilon_1\epsilon_2\epsilon_1$	$\epsilon_2\epsilon_1\epsilon_2\epsilon_3^{(+)}$	$\epsilon_2\epsilon_3\epsilon_2\epsilon_3$	$\epsilon_2\epsilon_3\epsilon_2\epsilon_1^{(-)}$	$\epsilon_2\epsilon_1\epsilon_2\epsilon_1$	$\epsilon_2\epsilon_1\epsilon_1\epsilon_1^{(+)}$	$\epsilon_1\epsilon_1$
$\epsilon_4\epsilon_3$	$\epsilon_4\epsilon_3\epsilon_4\epsilon_3$	$\epsilon_4\epsilon_3\epsilon_2\epsilon_3^{(+)}$	$\epsilon_2\epsilon_3\epsilon_2\epsilon_3$	$\epsilon_2\epsilon_3\epsilon_2\epsilon_1^{(-)}$	$\epsilon_2\epsilon_1\epsilon_2\epsilon_1$	$\epsilon_2\epsilon_1\epsilon_1\epsilon_1^{(+)}$	$\epsilon_1\epsilon_1$
$\epsilon_5\epsilon_3$	$\epsilon_5\epsilon_3\epsilon_5\epsilon_3$	$\epsilon_5\epsilon_3\epsilon_2\epsilon_3^{(+)}$	$\epsilon_2\epsilon_3\epsilon_2\epsilon_3$	$\epsilon_2\epsilon_3\epsilon_2\epsilon_1^{(-)}$	$\epsilon_2\epsilon_1\epsilon_2\epsilon_1$	$\epsilon_2\epsilon_1\epsilon_1\epsilon_1^{(+)}$	$\epsilon_1\epsilon_1$
$\epsilon_6\epsilon_3$	$\epsilon_6\epsilon_3\epsilon_6\epsilon_3$	$\epsilon_6\epsilon_3\epsilon_2\epsilon_3^{(+)}$	$\epsilon_2\epsilon_3\epsilon_2\epsilon_3$	$\epsilon_2\epsilon_3\epsilon_2\epsilon_1^{(-)}$	$\epsilon_2\epsilon_1\epsilon_2\epsilon_1$	$\epsilon_2\epsilon_1\epsilon_1\epsilon_1^{(+)}$	$\epsilon_1\epsilon_1$
$\epsilon_4\epsilon_2$	$\epsilon_4\epsilon_2\epsilon_4\epsilon_2$	$\epsilon_4\epsilon_2\epsilon_4\epsilon_1^{(-)}$	$\epsilon_4\epsilon_1\epsilon_4\epsilon_1$	$\epsilon_4\epsilon_1\epsilon_2\epsilon_1^{(+)}$	$\epsilon_2\epsilon_1\epsilon_2\epsilon_1$	$\epsilon_2\epsilon_1\epsilon_1\epsilon_1^{(+)}$	$\epsilon_1\epsilon_1$
$\epsilon_4\epsilon_3$	$\epsilon_4\epsilon_3\epsilon_4\epsilon_3$	$\epsilon_4\epsilon_3\epsilon_4\epsilon_1^{(-)}$	$\epsilon_4\epsilon_1\epsilon_4\epsilon_1$	$\epsilon_4\epsilon_1\epsilon_2\epsilon_1^{(+)}$	$\epsilon_2\epsilon_1\epsilon_2\epsilon_1$	$\epsilon_2\epsilon_1\epsilon_1\epsilon_1^{(+)}$	$\epsilon_1\epsilon_1$
$\epsilon_2\epsilon_1$	$\epsilon_2\epsilon_1\epsilon_2\epsilon_1$	$\epsilon_2\epsilon_1\epsilon_4\epsilon_1^{(-)}$	$\epsilon_4\epsilon_1\epsilon_4\epsilon_1$	$\epsilon_4\epsilon_1\epsilon_2\epsilon_1^{(+)}$	$\epsilon_2\epsilon_1\epsilon_2\epsilon_1$	$\epsilon_2\epsilon_1\epsilon_1\epsilon_1^{(+)}$	$\epsilon_1\epsilon_1$
$\epsilon_3\epsilon_1$	$\epsilon_3\epsilon_1\epsilon_3\epsilon_1$	$\epsilon_3\epsilon_1\epsilon_4\epsilon_1^{(-)}$	$\epsilon_4\epsilon_1\epsilon_4\epsilon_1$	$\epsilon_4\epsilon_1\epsilon_2\epsilon_1^{(+)}$	$\epsilon_2\epsilon_1\epsilon_2\epsilon_1$	$\epsilon_2\epsilon_1\epsilon_1\epsilon_1^{(+)}$	$\epsilon_1\epsilon_1$
$\epsilon_5\epsilon_2$	$\epsilon_5\epsilon_2\epsilon_5\epsilon_2$	$\epsilon_5\epsilon_2\epsilon_5\epsilon_1^{(-)}$	$\epsilon_5\epsilon_1\epsilon_5\epsilon_1$	$\epsilon_5\epsilon_1\epsilon_2\epsilon_1^{(+)}$	$\epsilon_2\epsilon_1\epsilon_2\epsilon_1$	$\epsilon_2\epsilon_1\epsilon_1\epsilon_1^{(+)}$	$\epsilon_1\epsilon_1$
$\epsilon_5\epsilon_3$	$\epsilon_5\epsilon_3\epsilon_5\epsilon_3$	$\epsilon_5\epsilon_3\epsilon_5\epsilon_1^{(-)}$	$\epsilon_5\epsilon_1\epsilon_5\epsilon_1$	$\epsilon_5\epsilon_1\epsilon_2\epsilon_1^{(+)}$	$\epsilon_2\epsilon_1\epsilon_2\epsilon_1$	$\epsilon_2\epsilon_1\epsilon_1\epsilon_1^{(+)}$	$\epsilon_1\epsilon_1$
$\epsilon_2\epsilon_1$	$\epsilon_2\epsilon_1\epsilon_2\epsilon_1$	$\epsilon_2\epsilon_1\epsilon_5\epsilon_1^{(-)}$	$\epsilon_5\epsilon_1\epsilon_5\epsilon_1$	$\epsilon_5\epsilon_1\epsilon_2\epsilon_1^{(+)}$	$\epsilon_2\epsilon_1\epsilon_2\epsilon_1$	$\epsilon_2\epsilon_1\epsilon_1\epsilon_1^{(+)}$	$\epsilon_1\epsilon_1$
$\epsilon_3\epsilon_1$	$\epsilon_3\epsilon_1\epsilon_3\epsilon_1$	$\epsilon_3\epsilon_1\epsilon_5\epsilon_1^{(-)}$	$\epsilon_5\epsilon_1\epsilon_5\epsilon_1$	$\epsilon_5\epsilon_1\epsilon_2\epsilon_1^{(+)}$	$\epsilon_2\epsilon_1\epsilon_2\epsilon_1$	$\epsilon_2\epsilon_1\epsilon_1\epsilon_1^{(+)}$	$\epsilon_1\epsilon_1$
$\epsilon_6\epsilon_2$	$\epsilon_6\epsilon_2\epsilon_6\epsilon_2$	$\epsilon_6\epsilon_2\epsilon_6\epsilon_1^{(-)}$	$\epsilon_6\epsilon_1\epsilon_6\epsilon_1$	$\epsilon_6\epsilon_1\epsilon_2\epsilon_1^{(+)}$	$\epsilon_2\epsilon_1\epsilon_2\epsilon_1$	$\epsilon_2\epsilon_1\epsilon_1\epsilon_1^{(+)}$	$\epsilon_1\epsilon_1$
$\epsilon_6\epsilon_3$	$\epsilon_6\epsilon_3\epsilon_6\epsilon_3$	$\epsilon_6\epsilon_3\epsilon_6\epsilon_1^{(-)}$	$\epsilon_6\epsilon_1\epsilon_6\epsilon_1$	$\epsilon_6\epsilon_1\epsilon_2\epsilon_1^{(+)}$	$\epsilon_2\epsilon_1\epsilon_2\epsilon_1$	$\epsilon_2\epsilon_1\epsilon_1\epsilon_1^{(+)}$	$\epsilon_1\epsilon_1$
$\epsilon_2\epsilon_1$	$\epsilon_2\epsilon_1\epsilon_2\epsilon_1$	$\epsilon_2\epsilon_1\epsilon_6\epsilon_1^{(-)}$	$\epsilon_6\epsilon_1\epsilon_6\epsilon_1$	$\epsilon_6\epsilon_1\epsilon_2\epsilon_1^{(+)}$	$\epsilon_2\epsilon_1\epsilon_2\epsilon_1$	$\epsilon_2\epsilon_1\epsilon_1\epsilon_1^{(+)}$	$\epsilon_1\epsilon_1$
$\epsilon_3\epsilon_1$	$\epsilon_3\epsilon_1\epsilon_3\epsilon_1$	$\epsilon_3\epsilon_1\epsilon_6\epsilon_1^{(-)}$	$\epsilon_6\epsilon_1\epsilon_6\epsilon_1$	$\epsilon_6\epsilon_1\epsilon_2\epsilon_1^{(+)}$	$\epsilon_2\epsilon_1\epsilon_2\epsilon_1$	$\epsilon_2\epsilon_1\epsilon_1\epsilon_1^{(+)}$	$\epsilon_1\epsilon_1$
$\epsilon_2\epsilon_1$	$\epsilon_2\epsilon_1\epsilon_2\epsilon_1$	$\epsilon_2\epsilon_1\epsilon_1\epsilon_1^{(+)}$	$\epsilon_1\epsilon_1\epsilon_1\epsilon_1$	$\epsilon_1\epsilon_1\epsilon_3\epsilon_1^{(-)}$	$\epsilon_3\epsilon_1\epsilon_3\epsilon_1$	$\epsilon_3\epsilon_1\epsilon_1\epsilon_1^{(+)}$	$\epsilon_1\epsilon_1$
$\epsilon_3\epsilon_1$	$\epsilon_3\epsilon_1\epsilon_3\epsilon_1$	$\epsilon_3\epsilon_1\epsilon_1\epsilon_1^{(+)}$	$\epsilon_1\epsilon_1\epsilon_1\epsilon_1$	$\epsilon_1\epsilon_1\epsilon_3\epsilon_1^{(-)}$	$\epsilon_3\epsilon_1\epsilon_3\epsilon_1$	$\epsilon_3\epsilon_1\epsilon_1\epsilon_1^{(+)}$	$\epsilon_1\epsilon_1$

TABLE I. (*Continued.*)

$\rho(t)$	$G(t-\tau_3)$	$L_{v[p]}(\tau_3)$	$G(\tau_3-\tau_2)$	$L_{v[q]}(\tau_2)$	$G(\tau_2-\tau_1)$	$L_{v[r]}(\tau_1)$	$\rho(t_0)$
$\epsilon_3\epsilon_1$	$\epsilon_3\epsilon_1\epsilon_3\epsilon_1$	$\epsilon_3\epsilon_1\epsilon_3\epsilon_2{}^{(+)}$	$\epsilon_3\epsilon_2\epsilon_3\epsilon_2$	$\epsilon_3\epsilon_2\epsilon_3\epsilon_1{}^{(-)}$	$\epsilon_3\epsilon_1\epsilon_3\epsilon_1$	$\epsilon_3\epsilon_1\epsilon_1\epsilon_1{}^{(+)}$	$\epsilon_1\epsilon_1$
$\epsilon_4\epsilon_2$	$\epsilon_4\epsilon_2\epsilon_4\epsilon_2$	$\epsilon_4\epsilon_2\epsilon_3\epsilon_2{}^{(+)}$	$\epsilon_3\epsilon_2\epsilon_3\epsilon_2$	$\epsilon_3\epsilon_2\epsilon_3\epsilon_1{}^{(-)}$	$\epsilon_3\epsilon_1\epsilon_3\epsilon_1$	$\epsilon_3\epsilon_1\epsilon_1\epsilon_1{}^{(+)}$	$\epsilon_1\epsilon_1$
$\epsilon_5\epsilon_2$	$\epsilon_5\epsilon_2\epsilon_5\epsilon_2$	$\epsilon_5\epsilon_2\epsilon_3\epsilon_2{}^{(+)}$	$\epsilon_3\epsilon_2\epsilon_3\epsilon_2$	$\epsilon_3\epsilon_2\epsilon_3\epsilon_1{}^{(-)}$	$\epsilon_3\epsilon_1\epsilon_3\epsilon_1$	$\epsilon_3\epsilon_1\epsilon_1\epsilon_1{}^{(+)}$	$\epsilon_1\epsilon_1$
$\epsilon_6\epsilon_2$	$\epsilon_6\epsilon_2\epsilon_6\epsilon_2$	$\epsilon_6\epsilon_2\epsilon_3\epsilon_2{}^{(+)}$	$\epsilon_3\epsilon_2\epsilon_3\epsilon_2$	$\epsilon_3\epsilon_2\epsilon_3\epsilon_1{}^{(-)}$	$\epsilon_3\epsilon_1\epsilon_3\epsilon_1$	$\epsilon_3\epsilon_1\epsilon_1\epsilon_1{}^{(+)}$	$\epsilon_1\epsilon_1$
$\epsilon_3\epsilon_1$	$\epsilon_3\epsilon_1\epsilon_3\epsilon_1$	$\epsilon_3\epsilon_1\epsilon_3\epsilon_3{}^{(+)}$	$\epsilon_3\epsilon_3\epsilon_3\epsilon_3$	$\epsilon_3\epsilon_3\epsilon_3\epsilon_1{}^{(-)}$	$\epsilon_3\epsilon_1\epsilon_3\epsilon_1$	$\epsilon_3\epsilon_1\epsilon_1\epsilon_1{}^{(+)}$	$\epsilon_1\epsilon_1$
$\epsilon_4\epsilon_3$	$\epsilon_4\epsilon_3\epsilon_4\epsilon_3$	$\epsilon_4\epsilon_3\epsilon_3\epsilon_3{}^{(+)}$	$\epsilon_3\epsilon_3\epsilon_3\epsilon_3$	$\epsilon_3\epsilon_3\epsilon_3\epsilon_1{}^{(-)}$	$\epsilon_3\epsilon_1\epsilon_3\epsilon_1$	$\epsilon_3\epsilon_1\epsilon_1\epsilon_1{}^{(+)}$	$\epsilon_1\epsilon_1$
$\epsilon_5\epsilon_3$	$\epsilon_5\epsilon_3\epsilon_5\epsilon_3$	$\epsilon_5\epsilon_3\epsilon_3\epsilon_3{}^{(+)}$	$\epsilon_3\epsilon_3\epsilon_3\epsilon_3$	$\epsilon_3\epsilon_3\epsilon_3\epsilon_1{}^{(-)}$	$\epsilon_3\epsilon_1\epsilon_3\epsilon_1$	$\epsilon_3\epsilon_1\epsilon_1\epsilon_1{}^{(+)}$	$\epsilon_1\epsilon_1$
$\epsilon_6\epsilon_3$	$\epsilon_6\epsilon_3\epsilon_6\epsilon_3$	$\epsilon_6\epsilon_3\epsilon_3\epsilon_3{}^{(+)}$	$\epsilon_3\epsilon_3\epsilon_3\epsilon_3$	$\epsilon_3\epsilon_3\epsilon_3\epsilon_1{}^{(-)}$	$\epsilon_3\epsilon_1\epsilon_3\epsilon_1$	$\epsilon_3\epsilon_1\epsilon_1\epsilon_1{}^{(+)}$	$\epsilon_1\epsilon_1$
$\epsilon_4\epsilon_2$	$\epsilon_4\epsilon_2\epsilon_4\epsilon_2$	$\epsilon_4\epsilon_2\epsilon_4\epsilon_1{}^{(-)}$	$\epsilon_4\epsilon_1\epsilon_4\epsilon_1$	$\epsilon_4\epsilon_1\epsilon_3\epsilon_1{}^{(+)}$	$\epsilon_3\epsilon_1\epsilon_3\epsilon_1$	$\epsilon_3\epsilon_1\epsilon_1\epsilon_1{}^{(+)}$	$\epsilon_1\epsilon_1$
$\epsilon_4\epsilon_3$	$\epsilon_4\epsilon_3\epsilon_4\epsilon_3$	$\epsilon_4\epsilon_3\epsilon_4\epsilon_1{}^{(-)}$	$\epsilon_4\epsilon_1\epsilon_4\epsilon_1$	$\epsilon_4\epsilon_1\epsilon_3\epsilon_1{}^{(+)}$	$\epsilon_3\epsilon_1\epsilon_3\epsilon_1$	$\epsilon_3\epsilon_1\epsilon_1\epsilon_1{}^{(+)}$	$\epsilon_1\epsilon_1$
$\epsilon_2\epsilon_1$	$\epsilon_2\epsilon_1\epsilon_2\epsilon_1$	$\epsilon_2\epsilon_1\epsilon_4\epsilon_1{}^{(-)}$	$\epsilon_4\epsilon_1\epsilon_4\epsilon_1$	$\epsilon_4\epsilon_1\epsilon_3\epsilon_1{}^{(+)}$	$\epsilon_3\epsilon_1\epsilon_3\epsilon_1$	$\epsilon_3\epsilon_1\epsilon_1\epsilon_1{}^{(+)}$	$\epsilon_1\epsilon_1$
$\epsilon_3\epsilon_1$	$\epsilon_3\epsilon_1\epsilon_3\epsilon_1$	$\epsilon_3\epsilon_1\epsilon_4\epsilon_1{}^{(-)}$	$\epsilon_4\epsilon_1\epsilon_4\epsilon_1$	$\epsilon_4\epsilon_1\epsilon_3\epsilon_1{}^{(+)}$	$\epsilon_3\epsilon_1\epsilon_3\epsilon_1$	$\epsilon_3\epsilon_1\epsilon_1\epsilon_1{}^{(+)}$	$\epsilon_1\epsilon_1$
$\epsilon_5\epsilon_2$	$\epsilon_5\epsilon_2\epsilon_5\epsilon_2$	$\epsilon_5\epsilon_2\epsilon_5\epsilon_1{}^{(-)}$	$\epsilon_5\epsilon_1\epsilon_5\epsilon_1$	$\epsilon_5\epsilon_1\epsilon_3\epsilon_1{}^{(+)}$	$\epsilon_3\epsilon_1\epsilon_3\epsilon_1$	$\epsilon_3\epsilon_1\epsilon_1\epsilon_1{}^{(+)}$	$\epsilon_1\epsilon_1$
$\epsilon_5\epsilon_3$	$\epsilon_5\epsilon_3\epsilon_5\epsilon_3$	$\epsilon_5\epsilon_3\epsilon_5\epsilon_1{}^{(-)}$	$\epsilon_5\epsilon_1\epsilon_5\epsilon_1$	$\epsilon_5\epsilon_1\epsilon_3\epsilon_1{}^{(+)}$	$\epsilon_3\epsilon_1\epsilon_3\epsilon_1$	$\epsilon_3\epsilon_1\epsilon_1\epsilon_1{}^{(+)}$	$\epsilon_1\epsilon_1$
$\epsilon_2\epsilon_1$	$\epsilon_2\epsilon_1\epsilon_2\epsilon_1$	$\epsilon_2\epsilon_1\epsilon_5\epsilon_1{}^{(-)}$	$\epsilon_5\epsilon_1\epsilon_5\epsilon_1$	$\epsilon_5\epsilon_1\epsilon_3\epsilon_1{}^{(+)}$	$\epsilon_3\epsilon_1\epsilon_3\epsilon_1$	$\epsilon_3\epsilon_1\epsilon_1\epsilon_1{}^{(+)}$	$\epsilon_1\epsilon_1$
$\epsilon_3\epsilon_1$	$\epsilon_3\epsilon_1\epsilon_3\epsilon_1$	$\epsilon_3\epsilon_1\epsilon_5\epsilon_1{}^{(-)}$	$\epsilon_5\epsilon_1\epsilon_5\epsilon_1$	$\epsilon_5\epsilon_1\epsilon_3\epsilon_1{}^{(+)}$	$\epsilon_3\epsilon_1\epsilon_3\epsilon_1$	$\epsilon_3\epsilon_1\epsilon_1\epsilon_1{}^{(+)}$	$\epsilon_1\epsilon_1$
$\epsilon_6\epsilon_2$	$\epsilon_6\epsilon_2\epsilon_6\epsilon_2$	$\epsilon_6\epsilon_2\epsilon_6\epsilon_1{}^{(-)}$	$\epsilon_6\epsilon_1\epsilon_6\epsilon_1$	$\epsilon_6\epsilon_1\epsilon_3\epsilon_1{}^{(+)}$	$\epsilon_3\epsilon_1\epsilon_3\epsilon_1$	$\epsilon_3\epsilon_1\epsilon_1\epsilon_1{}^{(+)}$	$\epsilon_1\epsilon_1$
$\epsilon_6\epsilon_3$	$\epsilon_6\epsilon_3\epsilon_6\epsilon_3$	$\epsilon_6\epsilon_3\epsilon_6\epsilon_1{}^{(-)}$	$\epsilon_6\epsilon_1\epsilon_6\epsilon_1$	$\epsilon_6\epsilon_1\epsilon_3\epsilon_1{}^{(+)}$	$\epsilon_3\epsilon_1\epsilon_3\epsilon_1$	$\epsilon_3\epsilon_1\epsilon_1\epsilon_1{}^{(+)}$	$\epsilon_1\epsilon_1$
$\epsilon_2\epsilon_1$	$\epsilon_2\epsilon_1\epsilon_2\epsilon_1$	$\epsilon_2\epsilon_1\epsilon_6\epsilon_1{}^{(-)}$	$\epsilon_6\epsilon_1\epsilon_6\epsilon_1$	$\epsilon_6\epsilon_1\epsilon_3\epsilon_1{}^{(+)}$	$\epsilon_3\epsilon_1\epsilon_3\epsilon_1$	$\epsilon_3\epsilon_1\epsilon_1\epsilon_1{}^{(+)}$	$\epsilon_1\epsilon_1$
$\epsilon_3\epsilon_1$	$\epsilon_3\epsilon_1\epsilon_3\epsilon_1$	$\epsilon_3\epsilon_1\epsilon_6\epsilon_1{}^{(-)}$	$\epsilon_6\epsilon_1\epsilon_6\epsilon_1$	$\epsilon_6\epsilon_1\epsilon_3\epsilon_1{}^{(+)}$	$\epsilon_3\epsilon_1\epsilon_3\epsilon_1$	$\epsilon_3\epsilon_1\epsilon_1\epsilon_1{}^{(+)}$	$\epsilon_1\epsilon_1$

[1] S. Mukamel, *Principles of Nonlinear Optical Spectroscopy* (Oxford University Press, New York, 1995).
[2] S. Mukamel, Annu. Rev. Phys. Chem. **51**, 691 (2000).
[3] S. Mukamel and R. M. Hochstrasser, Chem. Phys. **266**, 135 (2001).
[4] S. Woutersen, Y. G. Mu, G. Stock, and P. Hamm, Proc. Natl. Acad. Sci. USA **98**, 11254 (2001).
[5] O. Golonzka, M. Khalil, N. Demirdöven, and A. Tokmakoff, J. Chem. Phys. **115**, 10814 (2001).
[6] G. C. Schatz and R. P. van Duyne, in *Handbook of Vibrational Spectroscopy*, edited by J. M. Chalmers and P. R. Griffiths (Wiley, Chichester, 2002).
[7] R. Jimenez, F. van Mourik, J. Y. Yu, and G. R. Fleming, J. Phys. Chem. B **101**, 7350 (1997).
[8] R. Agarwal, B. P. Krueger, G. D. Scholes, M. Yang, J. Yom, L. Mets, and G. R. Fleming, J. Phys. Chem. B **104**, 2908 (2000).
[9] K. Ohta, M. Yang, and G. R. Fleming, J. Chem. Phys. **115**, 7609 (2001).
[10] H. M. Vaswani, J. Stenger, P. Fromme, and G. R. Fleming, J. Phys. Chem. B **110**, 26303 (2006).
[11] T. Joo, Y. Jia, J. Yu, M. Lang, and G. R. Fleming, J. Chem. Phys. **104**, 6089 (1996).
[12] M. Cho, J. Yu, T. Joo, Y. Nagasawa, S. A. Passino, and G. R. Fleming, J. Phys. Chem. **100**, 11944 (1996).
[13] S. A. Passino, Y. Nagasawa, and G. R. Fleming, J. Chem. Phys. **107**, 6094 (1997).
[14] M. L. Groot, J. Yu, R. Agarwal, J. Norris, and G. R. Fleming, J. Phys. Chem. B **102**, 5923 (1998).
[15] B. S. Prall, D. Y. Parkinson, and G. R. Fleming, J. Chem. Phys. **123**, 054515 (2005).
[16] Y.-C. Chen, H. Lee, and G. R. Fleming, J. Phys. Chem. A **111**, 9499 (2007).
[17] T. Mancal and G. R. Fleming, J. Chem. Phys. **121**, 10556 (2004).
[18] M. Cho and G. R. Fleming, J. Chem. Phys. **123**, 114506 (2006).
[19] M. F. Gelin, D. Egorova, and W. Domcke, J. Chem. Phys. **123**, 164112 (2005).
[20] D. Egorova, M. F. Gelin, and W. Domcke, J. Chem. Phys. **126**, 074314 (2007).
[21] V. Chernyak and S. Mukamel, Phys. Rev. Lett. **74**, 4895 (1995).
[22] N. Christensson, T. Polivka, A. Yartsev, and T. Pullerits, Phys. Rev. B **79**, 245118 (2009).
[23] A. A. Villaeys, Y. J. Dappe, K. K. Liang, and S. H. Lin, Phys. Rev. A **79**, 053418 (2009).
[24] Y. Tanimura and S. Mukamel, J. Chem. Phys. **99**, 9496 (1993).
[25] T. Steffen, J. T. Fourkas, and K. Duppen, J. Chem. Phys. **105**, 7364 (1996).
[26] A. Tokmakoff, M. J. Lang, D. S. Larsen, G. R. Fleming, V. Chernyak, and S. Mukamel, Phys. Rev. Lett. **79**, 2702 (1997).
[27] S. Mukamel, A. Piryatinski, and V. Chernyak, Acc. Chem. Res. **32**, 145 (1999).
[28] A. Piryatinski, V. Chernyak, and S. Mukamel, Chem. Phys. **266**, 311 (2001).
[29] O. Golonzka and A. Tokmakoff, J. Chem. Phys. **115**, 297 (2001).
[30] O. Golonzka, M. Khalil, N. Demirdöven, and A. Tokmakoff, Phys. Rev. Lett. **86**, 2154 (2001).
[31] M. Cho, N. F. Scherer, G. R. Fleming, and S. Mukamel, J. Chem. Phys. **96**, 5618 (1992).
[32] Y. Tanimura and S. Mukamel, Phys. Rev. E **47**, 118 (1993).
[33] V. V. Lozovoy, I. Pastirk, M. G. Comstock, and M. Dantus, Chem. Phys. **266**, 205 (2001).
[34] E. Geva and J. L. Skinner, J. Chem. Phys. **107**, 7630 (1997).

[35] K. F. Everitt, E. Geva, and J. L. Skinner, J. Chem. Phys. **114**, 1326 (2001).
[36] K. F. Everitt and J. L. Skinner, Chem. Phys. **266**, 197 (2001).
[37] B. I. Grimberg, V. V. Lozovoy, M. Dantus, and S. Mukamel, J. Phys. Chem. A **106**, 697 (2002).
[38] V. V. Lozovoy, B. I. Grimberg, I. Pastirk, and M. Dantus, Chem. Phys. **267**, 99 (2001).
[39] M. Khalil and A. Tokmakoff, Chem. Phys. **266**, 213 (2001).
[40] D. W. Oxtoby and S. A. Rice, Chem. Phys. Lett. **42**, 1 (1976).
[41] J. T. Fourkas, H. Kawashima, and K. A. Nelson, J. Chem. Phys. **103**, 4393 (1995).